Marine and Petroleum Geology 73 (2016) 1–20

Contents lists available at ScienceDirect

Marine and Petroleum Geology

journal homepage: www.elsevier.com/locate/marpetgeo

Research paper

Use of borehole imaging to improve understanding of the in-situ stress orientation of Central and Northern England and its implications for unconventional hydrocarbon resources

Andrew Kingdon*, Mark W. Fellgett, John D.O. Williams

British Geological Survey, Environmental Science Centre, Nicker Hill, Keyworth, Nottingham, NG12 5GG, United Kingdom

ARTICLE INFO

Article history:
Received 7 July 2015
Received in revised form
15 January 2016
Accepted 7 February 2016
Available online 10 February 2016

Keywords:
In-situ stress
Petrophysics
Unconventional reservoirs
Fracking

ABSTRACT

New interest in the potential for shale gas in the United Kingdom (UK) has led to renewed exploration for hydrocarbons in the Carboniferous age Bowland–Hodder shales under Central and Northern England. Following an incidence of induced seismicity from hydraulic fracturing during 2010 at Preese Hall, Lancashire, the publically available databases quantifying the in-situ stress orientation of the United Kingdom have shown to be inadequate for safe planning and regulation of hydraulic fracturing. This paper therefore reappraises the in-situ stress orientation for central and northern England based wholly on new interpretations of high-resolution borehole imaging for stress indicators including borehole breakouts and drilling-induced tensile fractures. These analyses confirm the expected north northwest – south southeast orientation of maximum horizontal in-situ stress identified from previous studies (e.g. Evans and Brereton, 1990). The dual-caliper data generated by Evans and Brereton (1990) yields a mean S_{Hmax} orientation of 149.87° with a circular standard deviation of 66.9°. However the use of borehole imaging without incorporation of results from older dual-caliper logging tools very significantly decreases the associated uncertainty with a mean S_{Hmax} orientation of 150.9° with a circular standard deviation of 13.1°.

The use of high-resolution borehole imaging is thus shown to produce a more reliable assessment of in-situ stress orientation. The authors therefore recommend that the higher resolution of such imaging tools should therefore be treated as a de-facto standard for assessment of in-situ stress orientation prior to rock testing. Use of borehole imaging should be formally instituted into best practice or future regulations for assessment of in-situ stress orientation prior to any hydraulic fracturing operations in the UK.

1. Introduction

1.1. In-situ stress and unconventional hydrocarbons reservoirs

The first exploration well of a prospective shale-gas reservoir in the United Kingdom (UK) was drilled at Preese Hall (Lancashire) in 2010 to test the productivity of the Carboniferous Bowland Shale Formation (Andrews, 2013; Smith et al., 2010). Induced seismicity was experienced following hydraulic fracturing, culminating in a magnitude 2.3 ML earthquake (Green et al., 2012). Following this event, the UK government imposed a temporary suspension of the use of hydraulic fracturing whilst a review of safety and best practice was undertaken. Simultaneously, the Royal Society and Royal Academy of Engineering (Bickle et al., 2012) undertook a study of the state of knowledge around economic development of shale gas in the UK. A key conclusion of this review was that "the British Geological Survey should implement national surveys to characterise in-situ stresses and to identify faults affecting prospective UK shale plays". This statement recognised the poor state of knowledge of the in-situ stress in the UK, and identified the requirement for the review of data from which detailed information may be derived. The research reported in this paper is a direct response to that recommendation and is intended to establish best practice for future acquisition of data to fully understand in-situ stress orientations in the UK.

Understanding of the in-situ stress field is essential for successful and safe production of remaining UK hydrocarbon resources, particularly to the development of unconventional

* Corresponding author.
E-mail address: aki@bgs.ac.uk (A. Kingdon).

http://dx.doi.org/10.1016/j.marpetgeo.2016.02.012

reservoirs and shale horizons (Bickle et al., 2012). Knowledge of the in-situ stress orientation is important for understanding borehole stability, fluid flow in naturally-fractured reservoirs, and hydraulic fracture stimulation (Fuchs and Müller, 2001). Shale gas production typically involves hydraulic fracturing in deviated wells to increase the volume of produced gas (Bickle et al., 2012). The growth in gas and oil production from shale rocks that has taken place in the United States in the 21st century, has been a direct consequence of utilising hydraulic fracturing in deviated or horizontal wells. This creates a complex conductive fracture network allowing for an improvement in the well performance.

Shale gas production has potentially much greater impact on the population of the UK than in the US. Many of the major shale gas basins in the US are in sparsely populated areas. For example the Bakken Shale has predominantly been developed in North Dakota which has a population of 739,482 in 2014 with a population density of just 3.83 people/km^2 (U.S. Census Bureau, 2014). In contrast the much smaller area of northern and central England which overlies the potentially prospective Bowland Shale Formation includes several of England's largest cities with a total population of more than 14.6 million people, a population density of 502.7 people per km^2, over 100 times greater (Cartwright, 2015; Office for National Statistics, 2011). Any attempt to develop these resources in the UK therefore has the potential to affect a far greater number of people. Thus, improved understanding of the in-situ stress orientation in these parts of the UK is essential if shale gas exploitation is even to be considered, and should form any part of future regulations.

1.2. In-situ stress orientation

A critical factor in hydraulic fracturing operations is the orientation of the in-situ principal stresses. Hydraulic fracturing will propagate along the path of least resistance and create width in a direction that requires the least force. Therefore, hydraulic tensile fractures propagate parallel to the maximum horizontal stress (SHmax) in the vertical plane (Brudy and Zoback, 1999). Consequently, in order to maximise recovery with minimal energy input it is necessary to drill horizontal wells parallel to the minimum horizontal stress (S_{hmin}) direction. As a result hydraulic tensile fractures will propagate parallel to the maximum horizontal stress (S_{Hmax}) in the vertical plane (Brudy and Zoback, 1999). Understanding the orientation of the in-situ stress is therefore imperative prior to drilling in order to ensure that wells are deviated favorably with respect to the in-situ stress.

Previous work relating to UK in-situ stress orientation (Evans and Brereton, 1990) has been critically assessed as part of this study. This older study was undertaken using dual-caliper (also known as four arm caliper) logs analysed for the presence of borehole breakouts and will be shown to be inadequate for current needs. This paper therefore includes the first published account of the use of borehole image logs to characterise the orientation of S_{Hmax} onshore in the UK, across northern and central England, where borehole image logs are now available.

Fig. 1 shows the distribution of borehole imaging data across the UK, which by fortunate coincidence corresponds very closely to the area of the UK that is sub-cropped by the potentially economic Bowland–Hodder Shale. This also shows the dual-caliper data distribution across the UK.

1.3. Identifying stress field indicators

Bell and Gough (1979) noted that stress concentrations around vertical boreholes can cause caving, also known as a borehole breakout. Plumb and Hickman (1985) were able to show that the orientation of the elongations, or breakouts which result in a compressive failure of the well take place in the orientation of S_{hmin}, orthogonal to S_{Hmax} in vertical boreholes. For a more detailed description of breakout formation see Zoback et al. (1985). There are several wireline tools which can be used to identify borehole breakout which are discussed below.

1.3.1. Dual caliper logging

Dual-caliper logging, usually undertaken in conjunction with dipmeter tools typically measure four points on the borehole circumference with a vertical resolution of between 25 and 154 mm. Guidelines for breakout identification from caliper logs is detailed in Reinecker et al. (2003). The tool rotates as it is pulled up the wall however when it encounters a zone of borehole elongation the rotation will cease. The tool locks into an elongation zone which, with the aid of the other tool outputs, can be interpreted as a breakout (Reinecker et al., 2003).

1.3.2. Borehole imaging tools

Borehole imaging tools provide high resolution borehole images based on (generally) either ultrasonic velocity or resistivity. These tools and their origins are described in Paillet et al. (1990) and Prensky (1999). Borehole imaging tools provide wall coverage of between 20% and 95%, depending on the tool specification and borehole diameter. Table 1 describes the specific tool types used in this study and the details of their resolution (Ekstrom et al., 1987; Gaillot et al., 2007).

Tingay et al. (2008) investigated analysing borehole breakouts using image logging. They characterised borehole breakouts from resistivity image logs as parallel poorly resolved conductive zones that appear 180° apart on opposite sides of the borehole wall. However, the resolution of borehole breakouts is dependent on the width of the pad compared to the width of the breakout (Tingay et al., 2008). In a limited number of cases, resistivity images are accompanied by ultrasonic borehole images (e.g. Schlumberger's UBI™ tool) which circumferentially record both the amplitude and travel time of the returning wave form. These tools have lower vertical and angular resolution than the resistivity tools.

However, the travel time waveform (TTWF) images from acoustic logs are useful as they are more sensitive to changes in the borehole radius. In TTWF images breakouts appear as broad zones of increased borehole radius observed at 180° from one another (Tingay et al., 2008). Fig. 2 shows an example of resistivity (FMI) image and an acoustic (UBI) travel time image from the Sellafield 13A in Cumbria, highlighting the differences between the way these two types of tool show borehole breakout. In the absence of acoustic images, breakouts are therefore identified by darker (less conductive) patches on opposite sides of borehole images and a simultaneous disturbance to the spacing between the imaging pads.

1.4. Drilling induced tensile fractures

Whilst most fractures identifiable in boreholes are formed naturally, drilling induced tensile fractures (DIF's) result from tensile failure directly induced by the drilling process. These fractures form parallel to the orientation of the greatest far field horizontal stress (S_{HMAX}) (Moos and Zoback, 1990). These features occur when the sum circumferential stress concentration and the tensile strength are exceeded by the pressure in the well (Moos and Zoback, 1990). As DIF's have widths of only a few mm they can only be identified from high-resolution borehole image logs as they are not associated with any borehole enlargement (Tingay et al., 2008). They are generally narrow well defined features which are slightly inclined or sub-parallel to the borehole axis and form perpendicular to breakout orientation (Tingay et al., 2008). Fig. 3

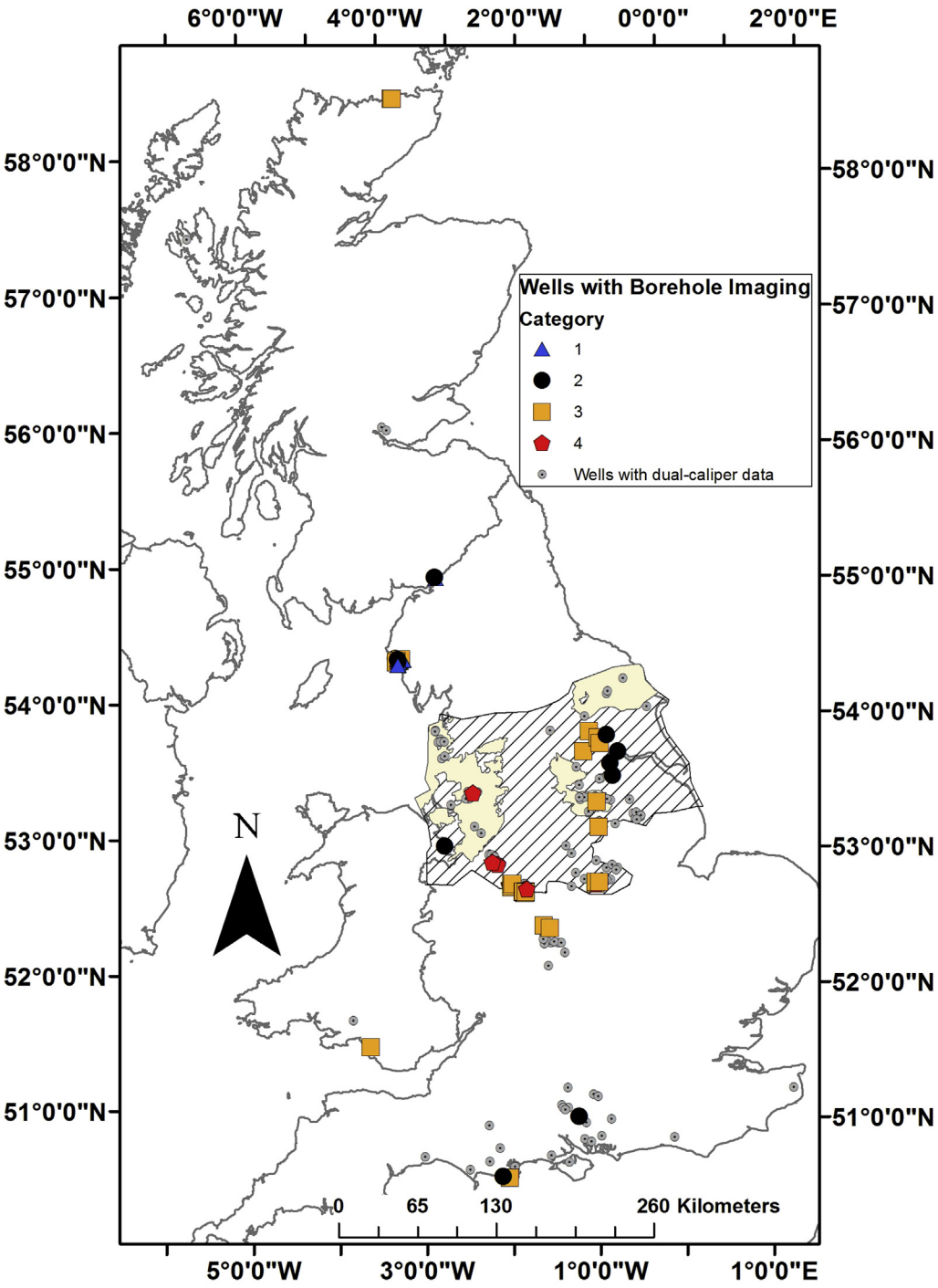

Fig. 1. Onshore map of distribution of wells logged with borehole imaging data by category across the UK compared with distribution of dual-caliper logs. Hatched zone is the area of interest for the BGS/DECC Bowland–Hodder Shale study area from Andrews (2013), solid fill shows the potentially prospective areas of the Bowland Shale Formation.

shows a section of the Melbourne 1 well in Yorkshire with both breakouts and tensile fractures.

2. Review of previous work

2.1. Borehole breakout studies

Systematic mapping of the S_{Hmax} orientation for UK onshore using downhole logs was principally conducted between 1989 and 1992 by the British Geological Survey (BGS) (Evans and Brereton, 1990). The work focused on the use of borehole breakouts to characterise the in-situ stress orientations using the eccentricity of dual-caliper log measurements to locate breakout intervals. Attempts to utilise resistivity eccentricity as a technique for identifying incipient breakouts (those that had not had time to form between the completion of drilling and subsequent logging operations), was ultimately unsuccessful and did not produce sufficiently reliable results to support their publication (Reeves, 2002).

Table 1
List of borehole imaging tools from which BGS holds digital data, details of tool specification, horizontal resolution and wall coverage.

Category	Company	Tool type	Tool names	Specifications	Approx. Vertical resolution	Approx. Coverage (8.5″ well)
1	Schlumberger	Resistivity & Acoustic	FMI & UBI	Tools run in combination	2.5 mm	100%
2	Schlumberger	Resistivity	FMI	192 button electrodes (24 per pad/flap × 4)	2.5 mm	80%
2	Schlumberger	Acoustic	UBI/BHTV/ATS	Rotating Sensor	5 mm	100%
2	Weatherford	Resistivity	CMI	176 button electrodes (20/24 per pad × 8)	2.5 mm	80%
2	Baker Hughes	Resistivity	STAR	144 button electrodes (12 × 6 pads)	5 mm	80%
3	Schlumberger	Resistivity	4-Pad FMS	64 button electrodes (16 × 4 pads)	2.5 mm	40%
4	Schlumberger	Resistivity	2-Pad FMS	58 button electrodes (29 × 2 pads)	2.5 mm	20%
5	Multiple	Dipmeter	Dual-Caliper	4 button electrodes (1 × 4 pads)	40 mm	>5%

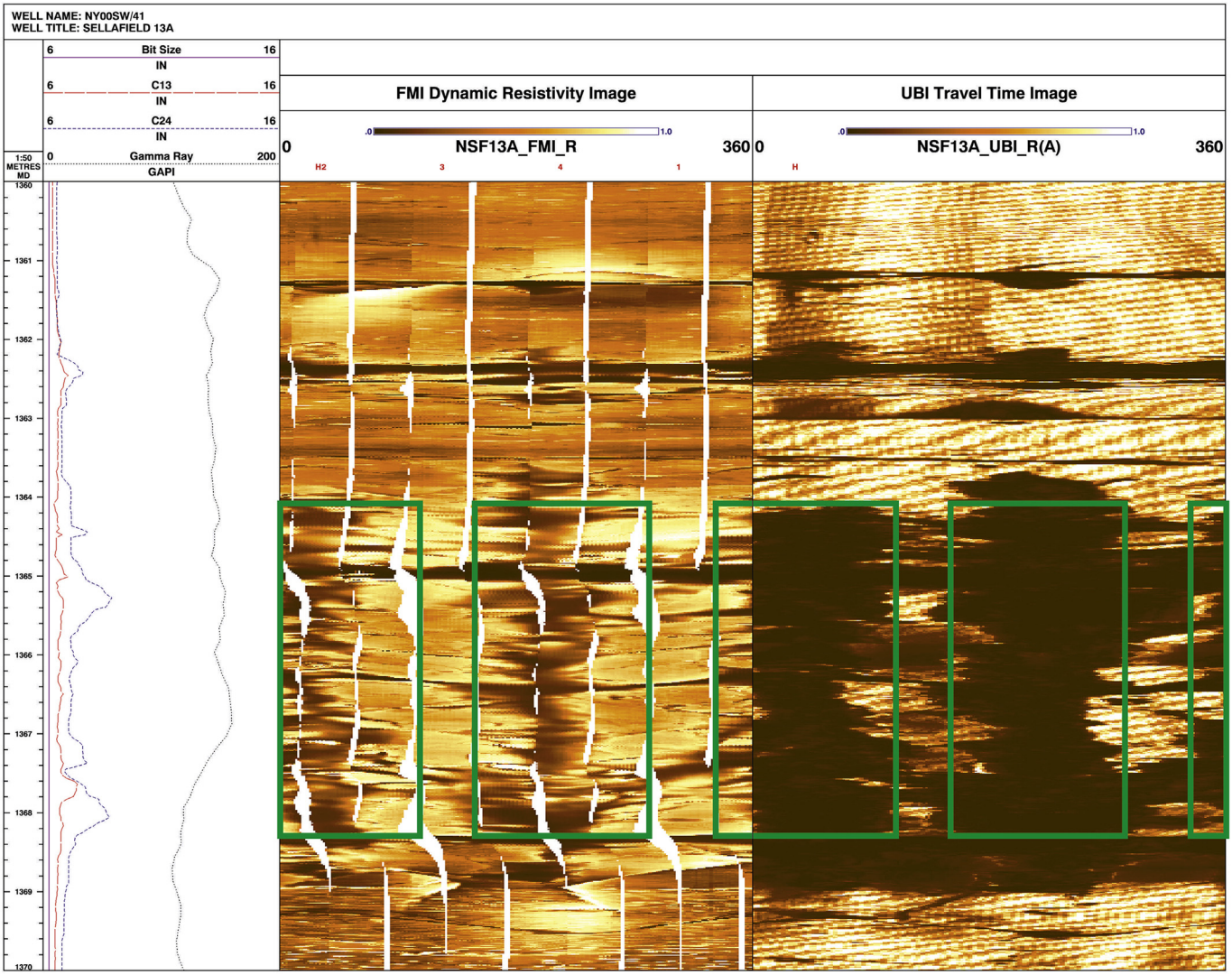

Fig. 2. Comparison of methods of visualising a 4 m long borehole breakout from St Bees Shale Formation, from borehole Sellafield 13A in Cumbria (10 m vertical borehole section). Left-hand panel: conventional logs including perpendicular dual-caliper and gamma-ray. Centre panel: Unwrapped circumferential resistivity borehole imaging (FMI) (clockwise from north) with breakout highlighted by the green boxes. Right panel: Unwrapped circumferential acoustic borehole amplitude imaging (UBI) (clockwise from north) with breakout highlighted by green boxes. (For interpretation of the references to colour in this figure legend, the reader is referred to the web version of this article.)

The stress field analysis was undertaken to improve understanding of the geothermal resources of the UK (Evans, 1987) and as part of preparatory studies for the creation of radioactive waste repositories (Brereton, 1991) to study the implications of stress anisotropy on the engineered structures (shafts, tunnels and waste disposal caverns) (e.g. Nirex, 1997). With the cessation of the UK radioactive waste disposal programme in 1997, such work was largely abandoned, and little effort has been afforded to the systematic mapping of in-situ stress orientations in the UK since, though recently the application to the study of fluid flow through critically stressed fractures in the repository environment was investigated (Sathar et al., 2012; Reeves, 2002).

The quality of the assessment by Evans and Brereton (1990) was hampered by the inadequacy of available data resources, software

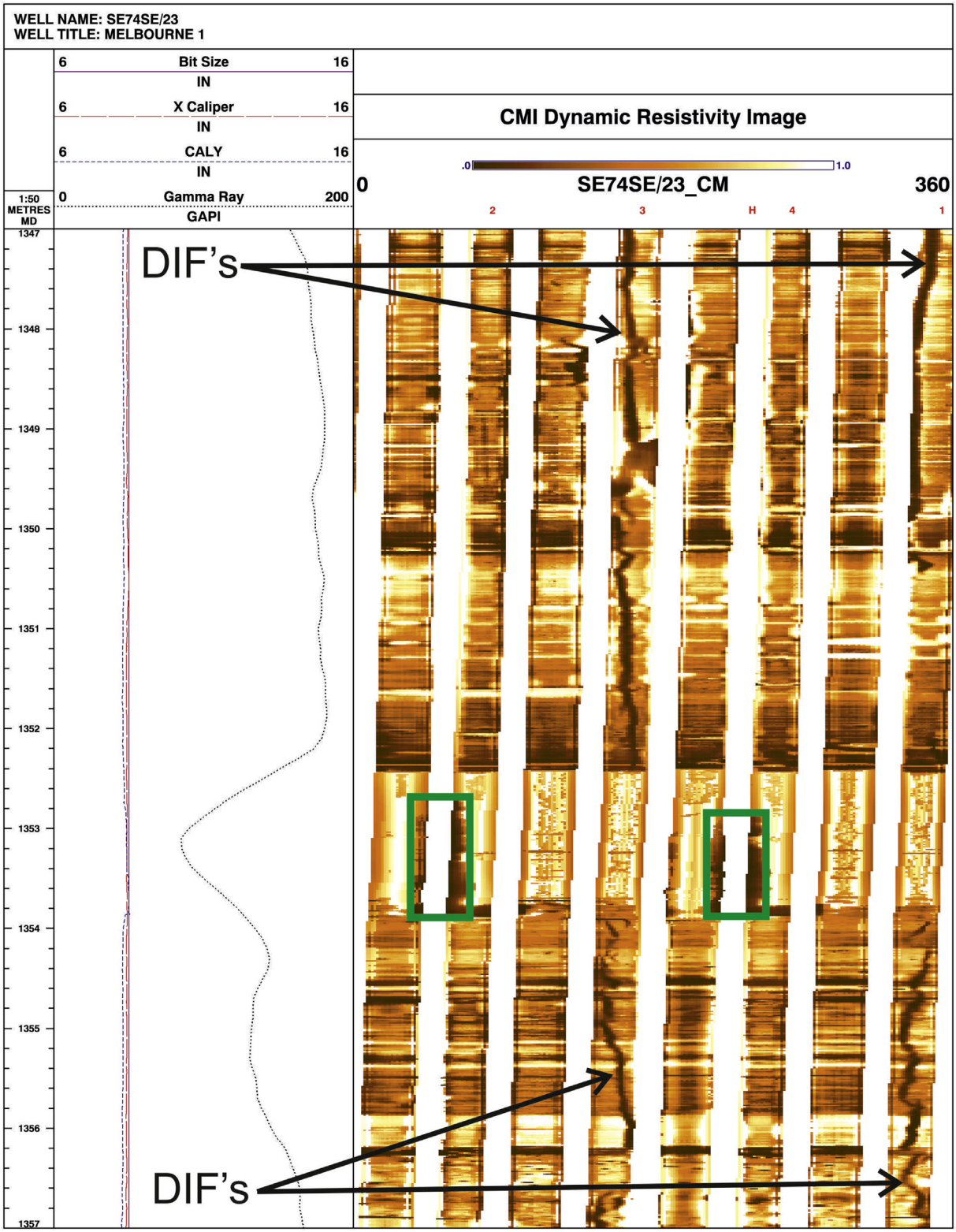

Fig. 3. Comparison of resistivity images visualising Drilling Induced tensile Fractures (DIFs) from PCM Measures in the Melbourne 1 well, Yorkshire (10 m vertical borehole section). Left-hand panel: conventional logs including perpendicular dual-caliper and gamma-ray log. Right: Unwrapped circumferential resistivity borehole imaging (CMI) (clockwise from north), breakouts highlighted by green boxes, DIFs terminate across coal horizon (lower gamma-ray) at 1352.4 m which shows clear breakout. (For interpretation of the references to colour in this figure legend, the reader is referred to the web version of this article.)

and some aspects of the methodological approach. Both the quality and quantity of dual-caliper data (from dipmeter tools) available was insufficient to deliver reliable stress orientations on the national scale. Evans and Brereton's (1990) technical workflow of the analysis is poorly documented and the high standard deviation indicates either poor data quality or analysis from the dual-caliper

logs. Therefore, replacement of these with more reliable datasets is required.

A broadly NW–SE orientation of S_{Hmax} is implied by the breakout analysis of Evans and Brereton (1990). Despite the shortcomings of the work, and the large degree of "noise" observed due to the inclusion of poorly characterised borehole features, this orientation is coincident with the NW–SE orientation expected in NW Europe due to the configuration of plate boundaries and associated tectonic ridge-push effects (Klein and Barr, 1986; Gölke and Coblentz, 1996). Borehole breakouts observed from dual-caliper and image logs have also been used to infer a similar and consistent orientation of S_{Hmax} in the UK southern North Sea (Williams et al., 2015). Some authors have used borehole breakout data to suggest that in the central and southern North Sea, thick and widespread Permian evaporites that have undergone significant halokinesis, may act to decouple the in-situ stress field, resulting in variable S_{Hmax} orientations in the shallowest sedimentary succession (Hillis and Nelson, 2005; Williams et al., 2014).

2.2. Overcoring studies

Interpretation of borehole breakouts is not the only method for identifying SHmax. Other techniques include overcoring which is often carried out in near horizontal holes using a sensor, based on the original design of Leeman and Hayes (1966). Overcoring methods measure in-situ stress based on stress relief around a hole. The relief of external forces by overcoring causes the changes in deformation. If the elastic rock properties are known the strain can be converted to in-situ stress in rock.

To take a measurement a pilot hole is drilled from the borehole wall in the unit of interest, a strain gauge is then inserted and cemented in place with resin. The gauge records a series of strain readings. The section around the pilot hole is then cored preserving the rock and the strain gauge. The core is then removed, the strain gauge measures the relaxation of the core and this can then be used to calculate the stresses acting on the core (Becker and Davenport, 2001). There are a considerable number of overcoring measurements for the UK landmass which are detailed in; Bigby et al. (1992); Cartwright (1997). However legacy overcoring data can be compromised with significant problems. The resin used to seal the strain gauge against the borehole wall can have poor adhesion and unreliable setting properties outside of laboratory conditions (Farmer and Kemeny, 1992). In addition to this, the overcoring method itself can also cause expansion of the adhesive, cell and rock due to induced heating. Furthermore, overcoring methods need accurate laboratory measurement of elastic rock properties such as trixial tests; if the rock is anisotropic such as coal, the stress issued from overcoring is uncertain. The result is that these techniques record a very high horizontal to vertical stress ratio which is exacerbated at shallow depths. For these reasons, the lack of recent studies, the shallow depths investigated and also the lack of critical review of the measurements the authors have chosen not to include this data in this work.

2.3. Focal mechanism studies

Analyses of principal horizontal stress orientations from across the globe have extensively used earthquake focal plane mechanisms. These are produced from the analysis of earthquakes, from which the fault plane solutions provide information on the crustal stresses. Baptie (2010) has undertaken such an analysis for the UK landmass, and suggests that strike-slip stress conditions with NW–SE compression predominate over much of the UK, while reverse faulting stress conditions with NE–SW compression dominate in Scotland to the north of the Midland Valley. Such earthquakes typically occur at depths greater than 3 km and often much deeper. Therefore in tectonically quiescent areas of the Earth such as the UK these may be of more limited relevance to understanding the in-situ stress orientations in the shallower geological succession.

2.4. World stress map

The World Stress Map (WSM) (Zoback et al., 1989; Heidbach et al., 2004, 2008) was initiated to produce 1:1 million continental-scale stress maps to provide information on the present day crustal stress field. In order to accomplish this, the WSM produced guidelines which have become de-facto standards for the identification of breakouts from dual-caliper logs (Reinecker et al., 2003) and borehole image logs (Tingey et al., 2008). Borehole breakouts comprise approximately 19% of the data in the WSM database, and are used alongside other data such as focal plane mechanisms to map the distribution of the global stress field (Tingay et al., 2008). The method for characterising borehole breakouts employed by the WSM concerns the identification of specific breakout intervals defined by a series of guidelines designed to minimise ambiguity. The WSM quality ranking scheme then enables collation with other datasets such as earthquake focal mechanisms to investigate basement stress orientations (Sperner et al., 2003), for example research on deep research boreholes such as Germany's KTB borehole (Emmermann and Lauterjung, 1997).

Once a well has been analysed for stress field indicators using the WSM guidelines it is then assigned a quality ranking (Heidbach et al., 2010). Table 2 presents the quality ranking scheme for borehole breakouts identified on image logs (Heidbach et al., 2010). Table 3 shows the equivalent quality ranking criteria for DIF's. The quality ranking system is valuable when collating crustal scale stress information (e.g. Heidbach et al., 2010).

2.5. Current UK stress orientation data

The most recent release of the WSM database (Heidbach et al., 2008) provides 53 S_{Hmax} orientations for the UK. Ten of these orientations are derived from borehole breakouts using variable input data from Nirex (1997) and Klein and Barr (1986). Measurements detailed in the most recent discussion of the WSM release (Heidbach et al., 2010) from across NW Europe generally support a NW–SE orientation of S_{Hmax}. The analysis of Evans and Brereton (1990) was not included in the WSM because of differences in methodology breakout identification. Evans and Brereton (1990) relied on a generalised view of the borehole data, rather than the identification of discrete breakout intervals.

Data currently available therefore includes a small number of published breakouts combined with a range of other stress indicators. These are insufficient for the decision making necessary for planning unconventional hydrocarbon reserves. Therefore there is a need for revision of the available UK datasets.

3. Methodology

3.1. Subsurface database

Previous work on the in-situ stress orientation of the UK was hampered by a paucity of data of sufficient quality to undertake a robust analysis. Since 1990, changes to BGS's role in managing geoscience data has meant that the quantity and quality of subsurface data now accessible far exceeds that which was available to Evans and Brereton (1990). Data are now available for almost all deep boreholes drilled to sample the subsurface and are archived

Table 2
Quality ranking scheme for borehole breakouts in a single well interpreted from image logs (Heidbach et al., 2010). S.D. denotes circular deviation after Mardia (1972).

A – quality	B – quality	C – quality	D – quality	E – quality
≥10 distinct breakout zones and combined length ≥100 m in a single well with S.D. ≤ 12°	≥6 distinct breakout zones and combined length of ≥40 m in a single well with S.D. ≤ 20°	≥4 distinct breakout zones and combined length ≥20 m in a single well with S.D. ≤ 25°	<4 distinct breakout zones or <20 m combined length with S.D. ≤ 40°	Wells without reliable breakouts or with S.D. > 40°

with BGS. Major datasets include all subsurface data from hydrocarbons exploration wells, the archives of both the UK Coal Authority and radioactive waste disposal program plus geothermal energy resources. Many of these datasets include petrophysical data, whilst some incorporate high-quality borehole imaging.

BGS has access to an extensive high quality petrophysical dataset with considerable borehole imaging, facilitating high resolution studies of in-situ stress orientation. Significant efforts have been expended to improve the data management of petrophysical log data in digital databases in the UK, including:

- Review and correction of metadata to ensure that all are properly located and orientated.
- Addition of borehole construction metadata, to include casing intervals and downhole bit size, allowing for accurate section-by-section review of borehole data.
- Where possible, inclinometry surveys from borehole image logs have been reloaded from original media to maximise availability and auditability.
- Review of all available data to ensure that any previously unidentified image logs are included and processed. Significant numbers of UK Coal Authority 2- and 4-pad FMS (Formation MicroScanner, please see Table 1) data were poorly archived but have now been re-read from magnetic media.
- Loading of the complete available digital archive of both the UK radioactive waste disposal programme of the 1990s and also the UK oil and gas industry which includes outputs from a variety of borehole imaging tools from the late 1980s up to recent data releases.

The current available image log database therefore constitutes the complete available (released) dataset of this type for the UK onshore area. While dual-caliper data are widely available (around 300 boreholes) covering more of the UK landmass it was of highly variable quality. Review of the geophysical log archive identified borehole imaging data for 85 boreholes concentrated in specific areas of the UK. Much of the data is concentrated in the area around the Pennines in central and northern England. These were largely deployed to image Carboniferous Pennine Coal Measures Group (PCM) for coal reserve appraisal or to investigate small oil and gas fields with Carboniferous source rocks.

3.2. Choice of borehole imaging over dual caliper data

The primary driver for this re-interpretation of the UK in-situ stress orientation has been the possible development of unconventional gas reservoirs. Most of the data available for identifying stress field indicators (borehole imaging and dual caliper measurements) were collected for onshore energy exploration. Therefore these are concentrated on the economic strata of the UK. The area of greatest relevance is the prospective area of the Bowland Shale Formation, which for stratigraphic reasons largely coincides with the area from which the majority of wells with borehole imaging are located in the UK. Therefore this study concentrates only on breakouts interpreted from borehole imaging. Given the distribution of the available data, the decision not to include other stress field indicators (such as breakouts identified from dual-caliper logged wells) has in practice not reduced the spatial or stratigraphic coverage, other than the omission of a small number of wells in Southern England (Fig. 1). The suitability of dual-caliper logs to identify breakouts in UK stress conditions are discussed in section 5.2 below.

3.3. Quality control of borehole imaging

Borehole imaging logs enable individual borehole breakouts to be identified down to a size of less than 10 cm vertically. As a result, borehole imaging greatly increases the amount of data available for breakout identification when compared with other techniques for identifying breakouts (eg dual caliper logs) as well as providing information on the physical properties of the borehole wall Therefore this study concentrates on breakouts that are uniquely identified from borehole imaging, with confirmatory information provided by DIFs.

Application of borehole imaging tools to the study of boreholes breakouts has been undertaken by the WSM (Tingay et al., 2008). However, many previous studies have utilised image-derived breakouts but assessed these against standard WSM conventions, for example Tingay et al. (2010). Comparison of breakout data derived from interpretation of image logs is dependent upon the consistency of the different imaging tools in use. The imaging data for the UK landmass has been acquired using a number of different imaging tools and historical variants. While low stress anisotropy will not likely produce metre-scale breakouts, it is the contention of these authors that given the high resolution of the borehole image logs, breakouts at sub-metre scale can yield reliable stress orientations when the incidents of breakout themselves are unambiguously observed from the borehole images.

The borehole imaging surveys incorporated into this dataset are of highly variable quality both in terms of the specific tools used but also the quality of the images acquired. The quality of processed images is controlled by multiple factors, discussed in depth by

Table 3
Quality ranking scheme for drilling induced fractures from image logs (Heidback et al., 2010).

A – quality	B – quality	C – quality	D – quality	E – quality
≥10 distinct DIF zones and combined length ≥100 m in a single well with s.d. ≤ 12°	≥6 distinct DIF zones and combined length ≥40 m in a single well with s.d. ≤ 20°	≥4 distinct DIF zones and combined length ≥20 m in a single well with s.d. ≤ 40°	<4 distinct DIF zones or <20 m combined length with s.d. ≤ 40°	Wells without reliable DIFs or with s.d. > 40°

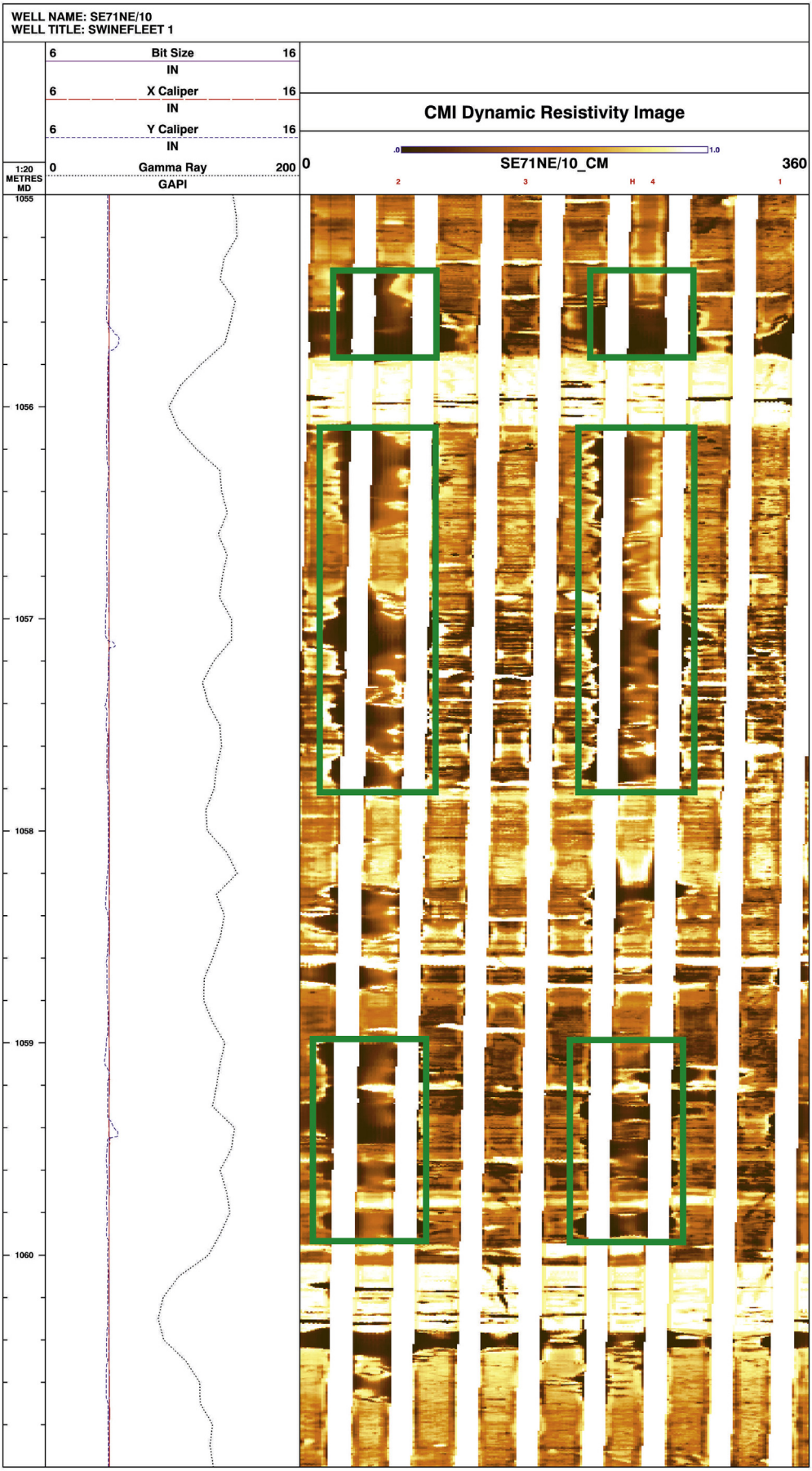
WELL NAME: SE71NE/10
WELL TITLE: SWINEFLEET 1
6 Bit Size 16
IN
6 X Caliper 16
IN
6 Y Caliper 16
IN
1:20
METRES
MD
0 Gamma Ray 200
GAPI
CMI Dynamic Resistivity Image
.0
1.0
0
SE71NE/10_CM
360
2
3
H
4
1
1055
1056
1057
1058
1059
1060

Garcia- Carballido et al. (2010) and by Evans et al. (2012). Therefore there is a highly heterogeneous quality to the available image log outputs and clarifying the exact model and specification of imaging tools is essential in evaluating the value that can be extracted from them. Since the work detailed in Evans and Brereton (1990), the use of borehole imaging tools has markedly increased, meaning an improved dataset is now available to aid in the interpretation of stress orientation.

The borehole imaging data held digitally by BGS reflects the development of imaging tools onshore in the UK over the past 30 years. From the use of the 2-pad FMS tool by the Coal Authority in the late 1980s to measure the vertical thickness of coal seams, to the FMI and CMI tools used today by the Oil and Gas industry. Table 1 gives a list of the imaging tools from which digital data are derived.

A specific aim of this study is to reduce the uncertainty in the SHmax orientation seen in previous work (Section 2.5) therefore clarity is required on the associated uncertainty of borehole imaging. Due to the diverse nature of data that is held, any features identified from image logs must be dealt with on a case by case basis. The data in the BGS archive mostly comprises resistivity imaging logs with acoustic logs available from only a small number of boreholes. Given that there is no consistent set of tools run for each well, five categories have been proposed which describe the borehole imaging data collected from each well and reflect the suitability of these tools to be used in breakout analysis. These categories are presented in Table 1.

Category 1 (e.g. Fig. 2) denotes micro resistivity tools with borehole wall coverage of ≥70% (in a borehole with an 8.5 inch diameter) and also an acoustic image with 100% coverage across 360°. Category 2 (e.g. Fig. 4) are micro resistivity tools with borehole wall coverage of ≥70% only. Category 3 (e.g. Fig. 5) are either a 4-pad micro-resistivity tool (which typically covers 25–40% of the borehole wall in an 8.5 inch hole) which has been run in conjunction with either an acoustic tool or a dual-caliper tool. Category 4 are 2-pad micro-resistivity tool in association with dual-caliper analysis from dipmeter tools. Category 5 only have dual-caliper analysis from dipmeter tool. Therefore the borehole breakouts identified from the Category 1 tools have higher certainty of orientation and a better chance of being imaged than those identified from Category 4 tools. Category 3 tools often identify breakouts but may not image the full width of the feature (Fig. 5) which Category 1 and 2 tools will accurately delineate, thereby increasing orientation certainty. This also allows shorter breakouts to be identified because the full outline of the feature is visible. In contrast, category 3 and 4 wells seldom capture the full breakout width thereby increasing uncertainty of orientation. Drilling Induced Tensile Fractures are much more likely to be identified on higher coverage tools (1 and 2) given their narrow width.

3.4. Interpretation of borehole images to identify breakouts

Identification of breakout features on borehole images is not a straightforward process because of the low wall coverage of many tools. With the exception of tools with both resistivity imaging and high quality acoustic imaging, most boreholes in the UK are reliant on resistivity images, and in most cases, where tools have less than 75% wall coverage. There is a high likelihood that the borehole image logs will fail to image the complete width of breakout features. Therefore identifying breakouts using such images is not a uniquely repeatable activity, but is to some degree subjective.

As can be seen in Fig. 2 the resistivity image clearly identifies the breakout but underestimates its width when compared with the true width shown on the travel time waveform image. Unfortunately high quality travel time imaging is rare in the UK. Fig. 4 shows a breakout from the Swinefleet 1 well in Yorkshire, identified using a static and dynamic resistivity image.

The methodology employed in this study involved the manual review and interpretation of all available borehole images in regular depth windows along the full length of each logged interval. All identified breakouts were subsequently reviewed by a separate interpreter, resulting in some breakouts being discarded. From the 85 boreholes from which data were available a number were eliminated for deviation of over 10° from vertical or because no breakouts were visible at the resolution given. Some 252 individual breakouts were identified in 36 wells across the UK. All boreholes in which breakouts were identified are within the northern and central England. Fig. 1 shows the spatial distribution of the 36 wells comprising the imaged borehole breakout dataset.

A major complexity in interpreting features of this scale is in ensuring that observed features are genuinely breakouts and not simply discrete zones of borehole wall damage unrelated to the in-situ stress regime. Therefore a variety of testing is required in order to ensure that the features are continuous. This has been achieved by carefully checking the vertical continuity of the breakout features.

Unless breakout features are so distinctive in the way that they are presented (Figs. 2–5), that they cannot be reasonably described as having any other cause then they should be identifiable over distinct vertical intervals, even if they are distributed discontinuously. Therefore even if intervals were very short then they were eligible for inclusion provided that there was clear evidence for other breakouts shown on that trend, even though some features may not be fully formed (that is they are seen as disturbances of the borehole wall at a constant orientation, but do not necessarily have clearly defined vertical limits).

Both Figs. 2 and 6 show zones of increased conductivity at 180° to each other conforming to the guidelines presented in Tingay et al. (2008). The increased resolution provided by image logging also allows for greater investigation of washout zones as seen in Fig. 7. Do you mean quality ranking here or your category ranking? This shows that washed-out units are not necessarily the upper and lower boundaries of borehole breakouts but may simply represent weaker units which have broken out and subsequently washed out during the drilling process.

Following observations from 12 wells with a borehole imaging category of 1 or 2, a minimum breakout length of 20 cm was set; 20 cm exceeds the standard logging interval (15 cm) so that geophysical log derived properties for these intervals could potentially be calculated to differentiate the physical properties of the breakout interval from the host rock.

For all breakouts the maximum hole deviation was set at 10° from vertical, a stipulation derived from work by Tingay et al. (2008). This project methodology is based on work by Mastin (1988) and is valid only when S_{Hmax} is not equal to S_{hmin} (This relates to normal and thrust faulting regimes). In normal and thrust faulting regimes if S_{Hmax} is approximately equal to S_{hmin} then there may be significant changes in breakout orientation in wells that are deviated by less than 10° (Mastin, 1988). The maximum deviation is

Fig. 4. Section of resistivity images visualising 3 distinct borehole breakouts from PCM from Swinefleet 1, Yorkshire (5 m vertical borehole section). Left-hand panel: conventional logs including perpendicular dual-caliper and gamma-ray log. Right panel: Unwrapped circumferential resistivity borehole imaging (CMI) (clockwise from north) with breakouts highlighted by green boxes. The breakouts on the borehole imaging are clear and distinct but these are not detected by the caliper tools. (For interpretation of the references to colour in this figure legend, the reader is referred to the web version of this article.)

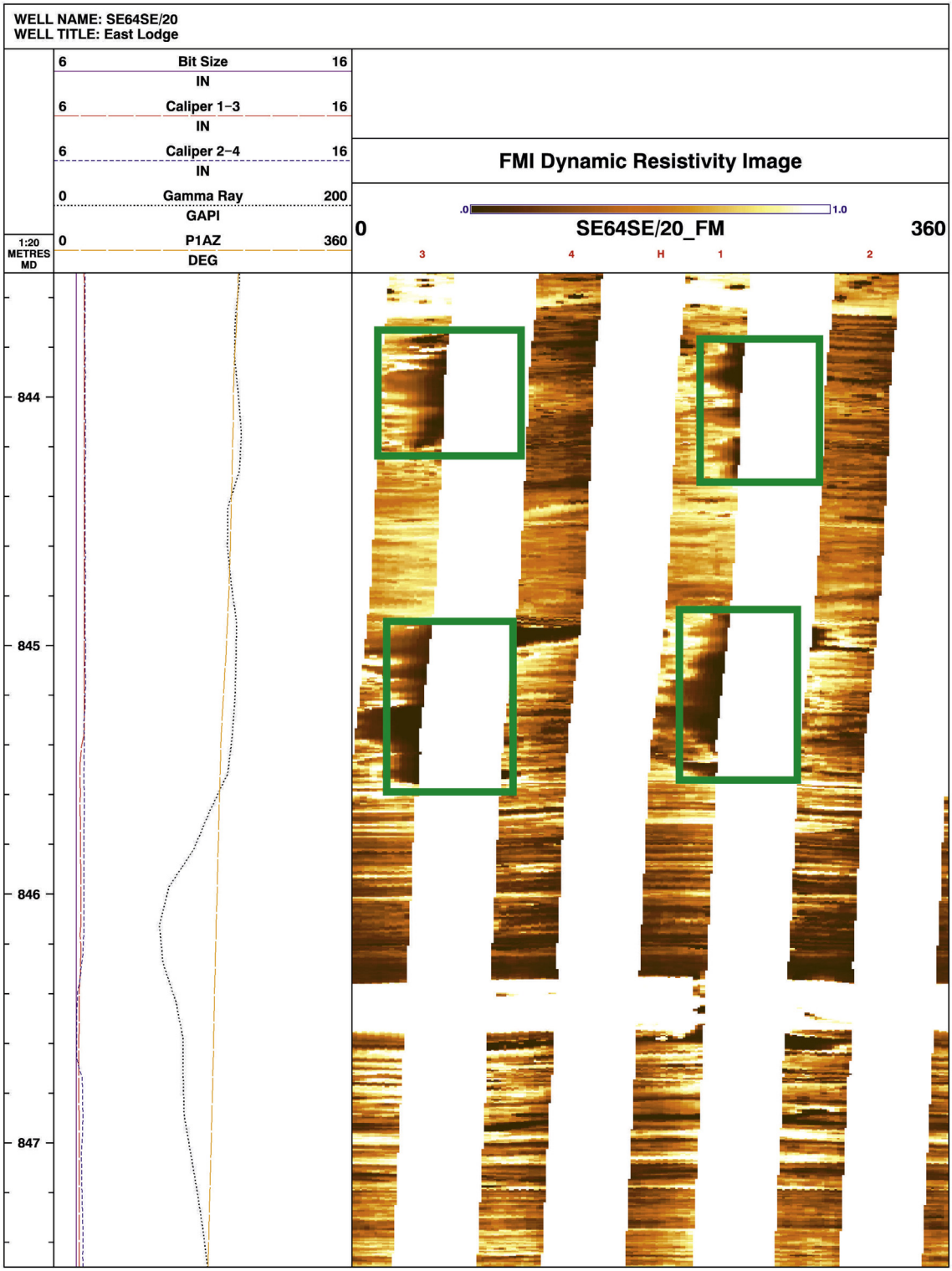

Fig. 5. Section of Category 3 resistivity images visualising a 0.8 m long borehole breakout from PCM, East Lodge borehole, Yorkshire (4 m vertical borehole section). Left-hand panel: conventional logs including perpendicular dual-caliper and gamma-ray log. Right: Unwrapped circumferential resistivity borehole imaging (FMS) (clockwise from north) with breakout highlighted by green boxes. Image highlights that this breakout would not satisfy a strict application of the WSM guidelines for breakout identification using caliper logs (Reinecker et al., 2003). The tool continues to rotate across the breakout interval, which is not marked by caliper enlargement. (For interpretation of the references to colour in this figure legend, the reader is referred to the web version of this article.)

intended specifically to prevent the characterisation of key seats as breakouts (Reinecker et al., 2003). Keyseats are features where damage occurs to the high side only of a deviated borehole. They are caused by direct wear from the drillstring on the borehole wall, this differentiates them from breakouts which show damage on opposite sides of the boreholes.

4. Results

4.1. Overall in-situ stress orientations

Fig. 8 shows the comparison of the newly interpreted image log data (left panel) compared with the total spread of data (right

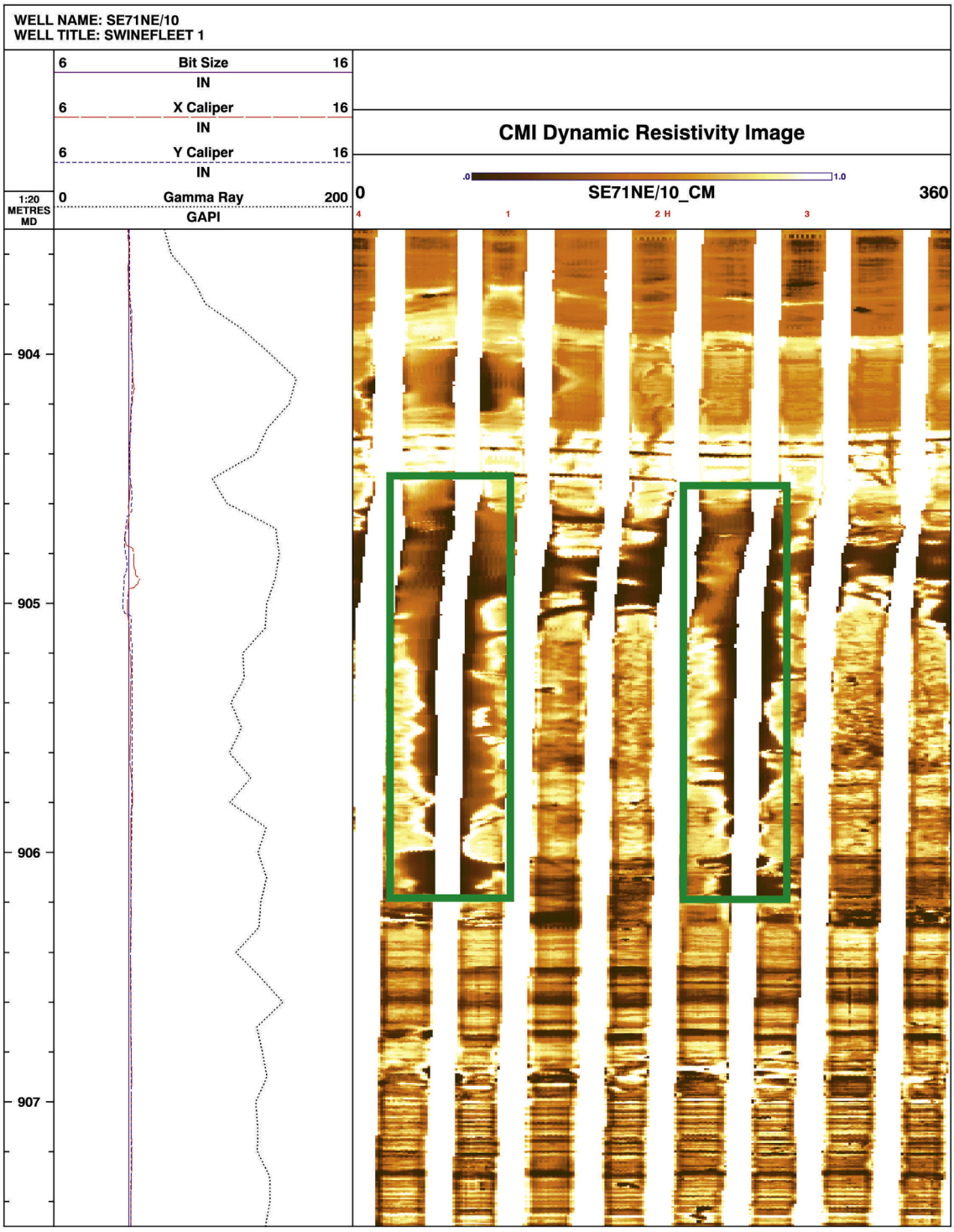

Fig. 6. Comparison of resistivity images visualising a 1.5 m long borehole breakout from PCM in Swinefleet 1, Yorkshire (4 m vertical borehole section). Left-hand panel: conventional logs including perpendicular dual-caliper and gamma-ray log. Right: Unwrapped circumferential resistivity borehole imaging (CMI) (clockwise from north) with 1.27 m breakout highlighted by green boxes. Image highlights that dual-caliper logs underestimate breakout size, length and complexity when compared with imaging. (For interpretation of the references to colour in this figure legend, the reader is referred to the web version of this article.)

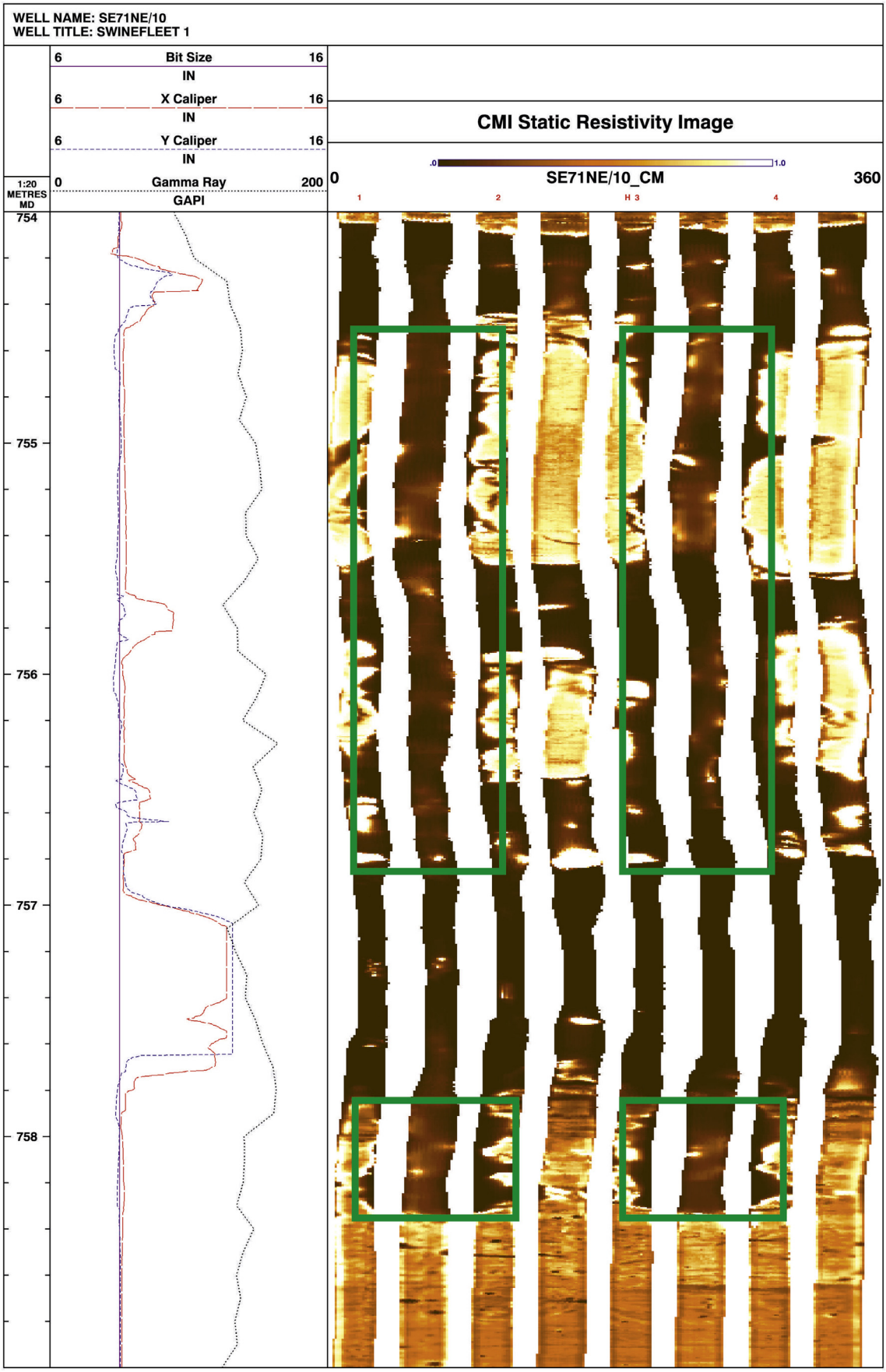
WELL NAME: SE71NE/10
WELL TITLE: SWINEFLEET 1
6 Bit Size 16
IN
6 X Caliper 16
IN
6 Y Caliper 16
IN
1:20
METRES
MD
0 Gamma Ray 200
GAPI
CMI Static Resistivity Image
.0 1.0
0 SE71NE/10_CM 360
1 2 H 3 4
754
755
756
757
758

panel) reported by Evans and Brereton (1990) interpreted solely from dual-caliper tools. For all of the maps (Figs. 9–12) S_{Hmax} orientations are plotted (breakout orientations ± 90°). The length of the petals on the rose diagrams are proportional to the number of observations per well.

Very clearly the dual caliper analyses have a completely circumferential scatter, on which a slight northwest-southeast trend is visible producing an S_{Hmax} direction of 149.87° with circular standard deviation of 66.9° calculated according to Mardia (1972). These vary markedly from the figures reported in Evans and Brereton (1990). This may indicate that the data that were reported were preferentially chosen to highlight the dominant orientation. The value quoted above is therefore calculated from the underpinning raw data files.

In significant contrast, the newly calculated data set has an S_{Hmax} orientation of 150.9° and circular standard deviation of 13.1°. This datasets shows a very clear trend with very limited associated scatter but contains all of the identified breakouts within the data interpreted within this study. Therefore the primary output of this study is the recognition that the exclusive use of borehole imaging tools has significantly reduced the uncertainty in the orientation of S_{Hmax}. Plainly, the interpretation of the borehole imaging tools produces a markedly more precise orientation of S_{Hmax} with reduced scatter. A metadata table for the list of wells presented in this paper is available in appendix A.

4.2. Area specific data analyses

An important aim of this study was to establish if the in-situ stress orientation observed on a national scale was markedly different than that observed on a regional basis. Therefore to understand the variability of S_{Hmax} at regional scales a number of discrete locations where examined. Each of these areas has a significant number of wells with borehole imaging.

Borehole breakouts were interpreted giving S_{Hmax} orientations.

4.2.1. Sellafield area stress analyses

The Sellafield investigation for siting a radioactive waste repository of the early 1990's included 26 resistivity and acoustically imaged boreholes. It should be noted that these were carefully drilled and extensively or completely cored, with drilling rates significantly lower than would be expected for equivalent depth hydrocarbon wells. Analysis of the caliper and borehole imaging logs shows that the walls of these boreholes are atypically smooth. The degree of micro-fracturing around the borehole circumference is therefore decreased which in turn minimises the propensity of the borehole wall to fail, making breakout formation less likely. Nonetheless these wells are important because these are the only example of a number of wells in a discrete area which have been separately analysed using the current methodology and were also analysed by Evans and Brereton. However it should be noted that the results for Sellafield were not reported in the 1990 paper due to the date of drilling and confidentiality issues.

Fig. 9 shows the in-situ stress orientation calculated for the Sellafield area boreholes using the Evans and Brereton (1990) methodology, as currently displayed on the BGS Rock Stress webpage (BGS, 2015) compared with the orientations interpreted by the authors. The Evans and Brereton (1990) work yields two dominant mean orientations of S_{Hmax}, NE–SW and roughly E–W. Borehole Sellafield 8A, the most north–eastern borehole shows a near circular stress "orientation".

All of the wells previously interpreted by Evans and Brereton were re-interpreted using the borehole imaging techniques detailed in this paper. Given the stricter methodology applied to breakout identification, unambiguous breakouts were identified in 6 of these wells, therefore other wells have been omitted. This shows a very clear NW–SE S_{Hmax} orientation across all but one of the wells. The Mean S_{Hmax} orientation is 154.5° with a circular standard deviation of 18.5° (Fig. 9). The single exception is RCF3. Despite RCF3 being a category 1 well, only a single breakout was identified and this may not be representative of the mean S_{Hmax} orientation along the length of the well. Data from RCF3 may suggest a localised rotation of the stress field caused by faulting identified in Nirex (1997).

4.2.2. Yorkshire and Midlands stress analyses

Figs. 10–12 show three regional stress maps showing S_{Hmax} orientations calculated from borehole imaging logs in Yorkshire (Fig. 10), West Staffordshire (Fig. 11) and the area around Lichfield (Fig. 12) respectively. These collectively account for in-situ stress orientation for some 22 of the total of 36 wells presented in this work with 172 of the 252 breakout observations shown. In almost all cases there is a clear NW–SE S_{Hmax} orientation which replicates that also visible in the data presented in Fig. 8.

Fig. 10 shows the rose diagrams of in-situ stress orientations from wells in Yorkshire. This map includes a number of recent (post 2005) image logged wells using the high-resolution Weatherford CMI logging tool. These wells have an average S_{Hmax} orientation of 147.5° and a circular standard deviation of 7.4°.

Fig. 11 shows a rose diagram of in-situ stress orientation of boreholes drilled in the West Staffordshire coalfield, to the west of Stoke-on-Trent derived from late 1980–90s vintage logging data. Fig. 12 show a rose diagram of in-situ stress orientation of boreholes drilled in the Warwickshire Coals field in the vicinity of Lichfield, again using late 1980–90s vintage logging data. The West Staffordshire wells show a mean S_{Hmax} orientation of 156.7° with a circular standard deviation of 10.7° and the Lichfield wells show a mean S_{Hmax} orientation of 158.8° with a circular standard deviation of 8.4°.

These wells were logged using both conventional 4-pad Schlumberger FMS (category 3) tools but also prototype 2-pad (category 4) tools. Given the low borehole wall coverage (typically >30%) of even 4-pad tool, identification of breakouts limited to highlighting zones of vertical disturbance with width assigned across these pads Therefore the actual breakout width is impossible to define; given that the pads will in all likelihood "lock-in" to the breakout orientation there is little likelihood that the full width of the breakout will be exposed across this interval. This is even more the case in the limited number of breakouts recorded from 2- pad FMS (category 4), these can only be used if confirmatory evidence is available such as breakouts interpreted in similar orientation from nearby wells. Therefore the very high degree of coincidence of the breakouts included in these two areas is to some extent an artefact of the logging tools used rather than completely a consequence of the natural variability of the breakout orientation (see Table 4).

Fig. 7. Comparison of resistivity images visualising borehole breakouts from PCM in the Swinefleet 1 well, Yorkshire (5 m vertical borehole section). Left-hand panel: conventional logs including perpendicular dual-caliper and gamma-ray log. Right: Unwrapped circumferential resistivity borehole imaging (CMI) (clockwise from north), breakouts highlighted by green boxes. This figure shows breakouts can be identified around washouts e.g. 180° the pale conductive zone (756.0–756.6 m) shown between darker "washed-out" zones with no caliper response. (For interpretation of the references to colour in this figure legend, the reader is referred to the web version of this article.)

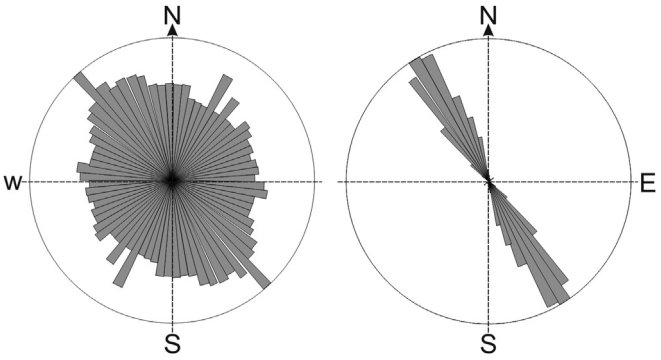

Fig. 8. Total S_{Hmax} orientation from borehole breakouts from two different study methods. Left panel: Summary Rose Diagram highlighting S_{Hmax} orientations from borehole breakout analysis derived from dual caliper tools only (Evans and Brereton, 1990) mean orientation 149.87° with a circular standard deviation of 66.9°. Right panel: Summary Rose Diagram highlighting S_{Hmax} orientations from borehole breakout analysis from this study derived from borehole imaging tools only, mean orientation 150.9° with circular standard deviation of 13.1°.

5. Discussion of the stress pattern and its implication for unconventional hydrocarbons

5.1. UK stress orientations

The results from the image log analysis of borehole breakouts (Table 4) presented in this paper clearly shows an SHmax orientation of NW–SE. This orientation is supported by earthquake focal plane mechanisms (Baptie, 2010) and the DIF dataset (Table 5). The results show no indication of regional or lithological changes suggested by Evans and Brereton (1990). However as shown in Fig. 1 the borehole imaging dataset presented is limited spatially but also stratigraphically.

5.2. Comparison of borehole imaging and dual-caliper data for identifying breakouts

Caliper logs are widely used for identifying breakouts in many locations globally, for example Reinecker et al., 2010; Reiter et al., 2014. Analysis was undertaken to assess the suitability of dual-caliper logs to identify borehole breakouts under UK stress conditions.

Four wells logged by borehole imaging were re-analysed using solely dual-caliper log data to determine whether these had sufficiently high resolution to accurately identify breakouts in UK stress conditions. These wells account for some 93 of the 252 breakouts presented in this paper.

These caliper logs were assessed against the WSM guidelines from Reinecker et al. (2003). These guidelines state that features can be classified as a possible breakout where one caliper closely matches bit size and the other diameter exceeds this by 10% e.g. in an 8.5 inch borehole, one diameter must exceed 9.35 inches to be breakout. These features must also be greater than 1 m in length. Almost all of the apparent breakouts identified from borehole imaging failed to be classified as caliper breakouts because they did not meet one or both of these guidelines. Fig. 13 shows four breakouts clearly visible on the borehole imaging. Whilst the caliper log apparently tracks these breakouts, two did not satisfy

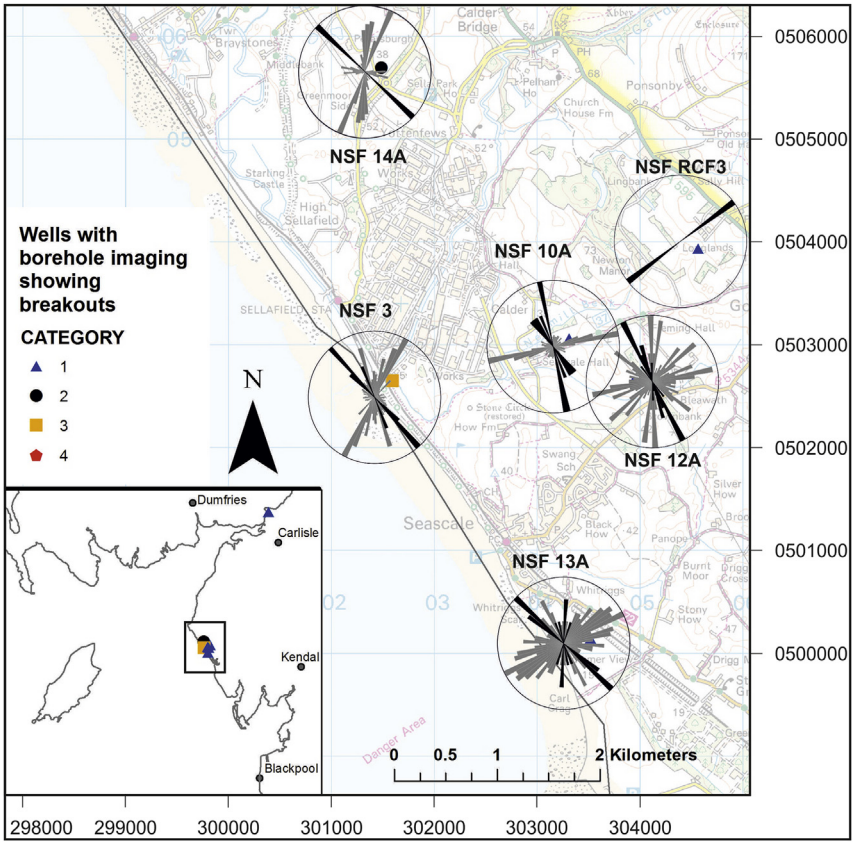

Fig. 9. Rose diagrams comparing stress field orientations from this study with Evans and Brereton (1990). Grey Rose diagrams show S_{Hmax} orientations identified from caliper eccentricity calculated by Evans and Brereton (1990) using dual-caliper eccentricity analysis. Black Rose diagrams showing S_{Hmax} orientations from borehole breakouts identified using borehole imaging tools in the Sellafield area of the UK, showing a mean S_{Hmax} orientation of 154.5° with a circular standard deviation of 18.5°.

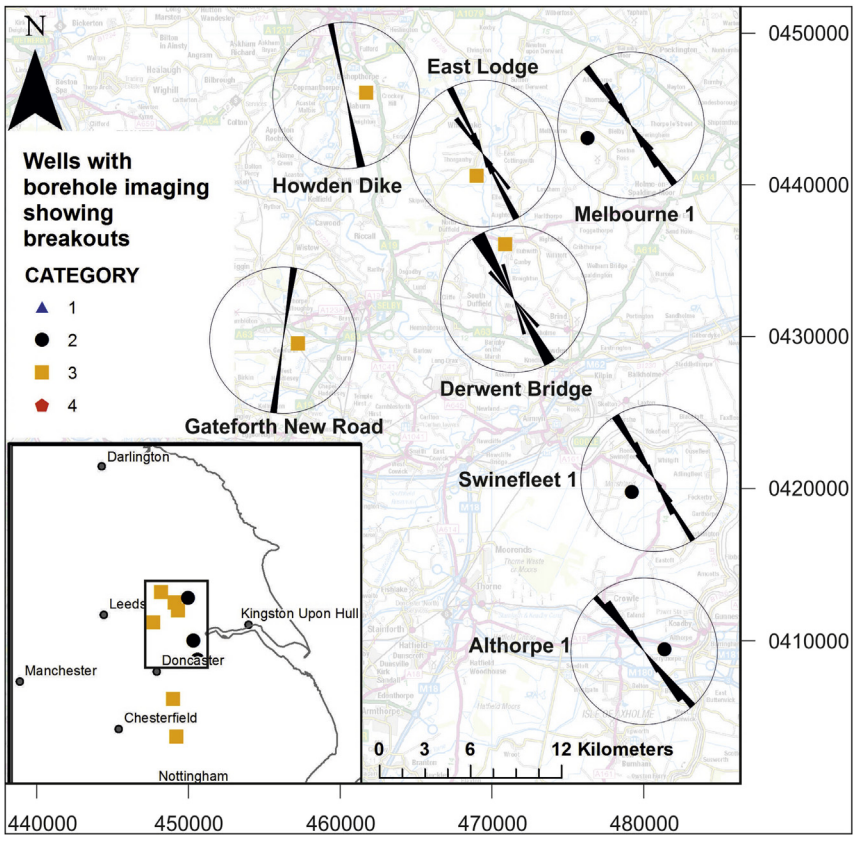

Fig. 10. Map highlighting orientations of S_{Hmax} derived from breakouts observed on borehole image logs for Yorkshire, showing a mean S_{Hmax} orientation of 147.5° with a circular standard deviation of 7.4°.

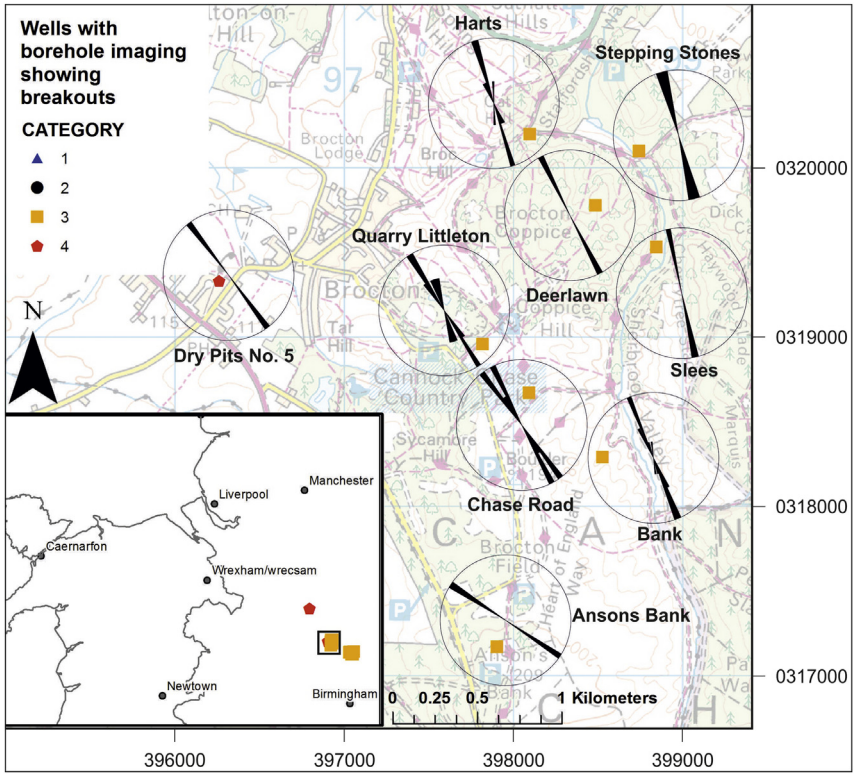

Fig. 11. Map highlighting orientations of S_{Hmax} derived from breakouts observed on borehole image logs for West Staffordshire, showing a mean S_{Hmax} orientation of 156.7° with a circular standard deviation of 10.7°.

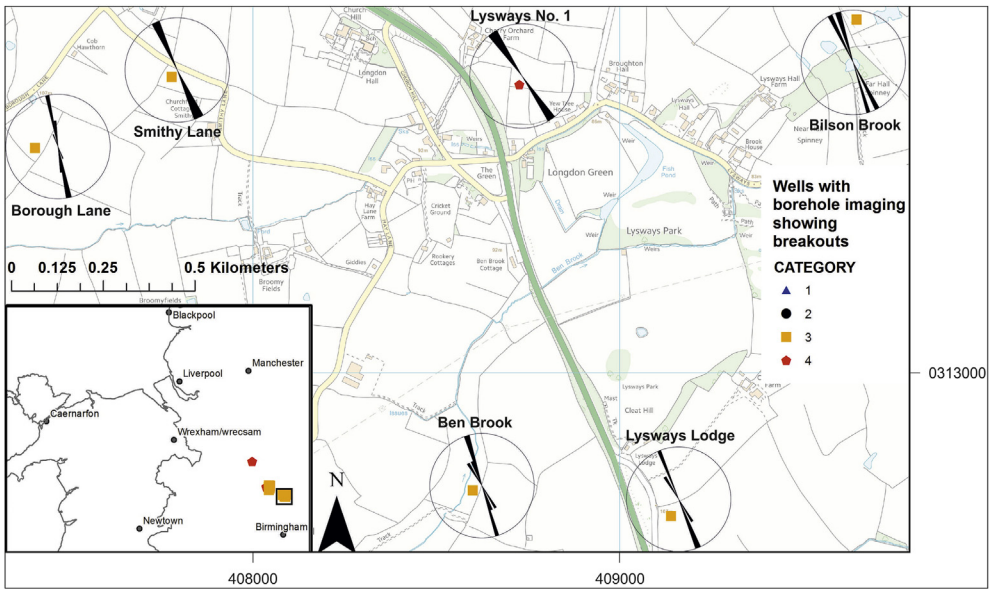

Fig. 12. Map highlighting orientations of S_{Hmax} derived from breakouts observed on borehole image logs for Lichfield area, showing a mean S_{Hmax} orientation of 158.8° with a circular standard deviation of 8.4°.

Table 4
Summary statistics for all breakouts identified using the borehole imaging technique. S.D. is the standard deviation calculated using the circular statistics of Mardia (1972).

Category	Number of breakouts	Mean angle (deg)	Variance (deg)	Circular S.D. (deg)	Orientation of S_{Hmax}	
1	45	66.83	9.2	16.95	156.83	336.83
2	84	55.94	1.89	7.42	145.94	325.94
3	110	63.58	6.76	14.35	153.58	333.58
4	3	54.92	0.93	5.17	144.92	324.92
Summary	252	60.91	5.66	13.07	150.91	330.91

Table 5
Summary statistics for all DIF's identified using the borehole imaging technique. S.D. is the standard deviation calculated using the circular statistics of Mardia (1972).

Category	Number of DIF's	Mean angle (deg)	Variance (deg)	Circular S.D. (deg)	Orientation of S_{Hmax}	
1	11	142.72	22.96	29.00	142.72	332.72
2	56	150.37	4.28	11.28	150.37	330.37
3	4	63.58	6.76	14.35	153.58	333.58
Summary	71	149.92	7.52	15.20	149.92	329.92

the 10% limit on increased diameter, and the remaining 2 were shorter than 1 m or even the reduced 0.5 m cut-off length adopted in Williams et al. (2015).

Of the 93 borehole imaging identified breakouts from these 4 wells, only 8 conformed to both guidelines; additional WSM guidelines about tool rotation were not even considered. Had these all been strictly applied then almost all borehole imaging identified breakouts would have been eliminated. Therefore any large scale analyses of dual-caliper logged wells would have be highly uncertain as it would be difficult to reliably separate breakouts from "noise". Therefore, it was decided that interpretation of wells logged only using the dual-caliper data should not be included as they are inadequate to reliably identify breakouts under UK stress conditions. Consequently they cannot be used to support robust decision making.

A first pass review of the caliper data for Southern England showed that so few wells contained clearly distinguishable breakouts as to make a more detailed interpretation of the available data not worthwhile. Williams et al. (2015) did use caliper logs for breakout identification in the Southern North Sea. However, very little borehole imaging was available and the wells sampled strata that are typically 500–1000 m deeper than those onshore.

5.3. Analysis of breakouts by depth

Fig. 14 shows a compilation of all of the recorded breakouts compiled by depth intervals binned in 500 m windows to investigate whether depth of the breakouts has any significant control of the in-situ stress orientation, the length of each sector is proportional to the numbers of breakouts in that direction. The most obvious conclusion from this is that there is little change in the dominant S_{Hmax} orientation with depth. Distribution of the numbers of breakout data per depth interval are summarised in Table 6. Whilst desirable, it was impractical to differentiate stress orientation by stratigraphy as UK borehole imaging logs are disproportionately collected from PCM, therefore statistical meaningful comparison with other stratigraphic units is not possible.

Table 4 shows the summary statistics for S_{Hmax} orientations derived from borehole breakouts calculated by well category and in

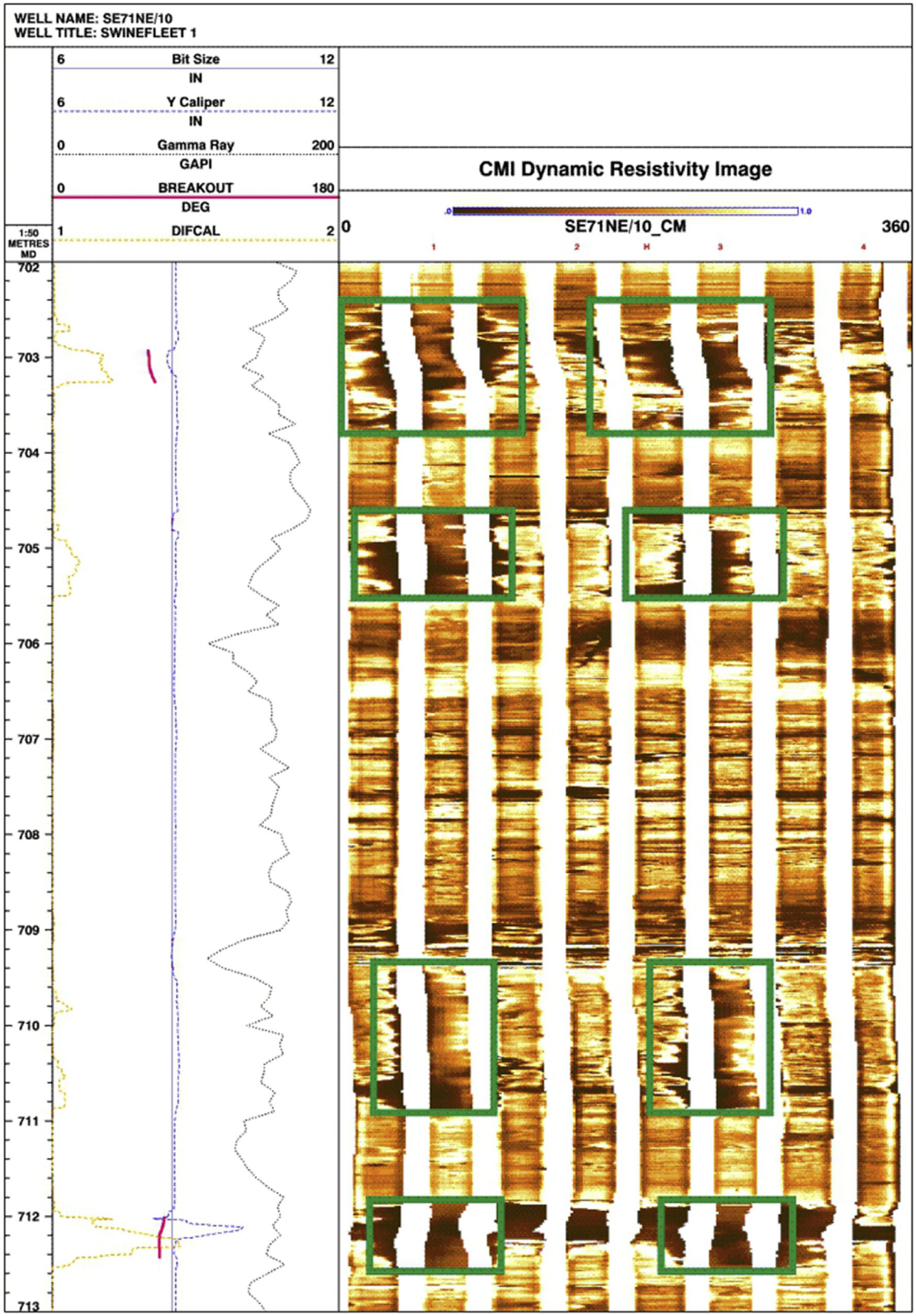

Fig. 13. Comparison of resistivity images highlighting 4 separate breakouts from PCM in the Swinefleet 1 well, Yorkshire (11 m vertical borehole section). Left-hand panel: conventional logs including differential caliper and gamma-ray log. Right: Unwrapped circumferential resistivity borehole imaging (CMI) (clockwise from north), breakouts highlighted by green boxes. Low gamma-ray silt facies separate breakout zones with higher gamma-ray/clay contents suggesting a strong degree of lithological control on breakout formation. Caliper eccentricity only exceeds bit size by 10% in two of the four breakout sections (Y caliper reads close to bit size). The two potential breakouts (in scarlet) identified using caliper eccentricity have a length < 50 cm. (For interpretation of the references to colour in this figure legend, the reader is referred to the web version of this article.)

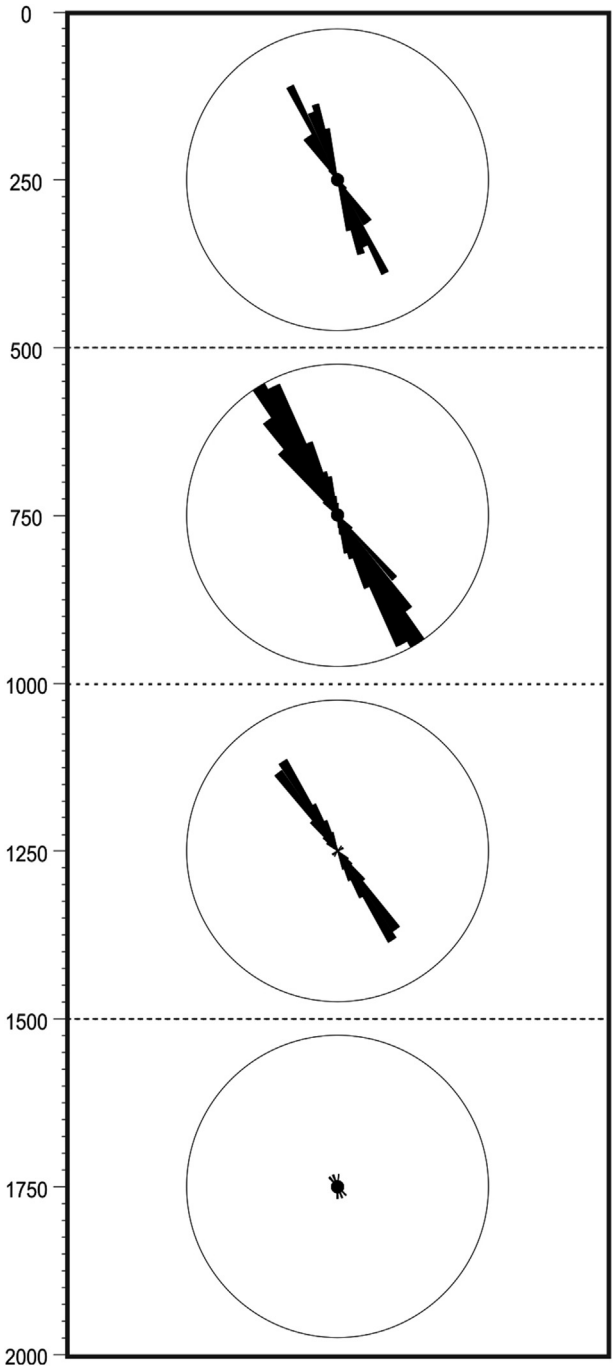

Fig. 14. Breakdown of breakout observations against depth from all 36 wells with interpreted breakouts presented in this paper, grouped in 500 m intervals. This highlights the shallow depth of borehole breakouts identified in this paper which contrasts with many studies incorporated into the most recent WSM data release (Heidbach et al., 2010); therefore the authors recommend that only borehole imaging tools will be able to identify the resulting breakouts.

total using the circular statistics of Mardia (1972). Table 5 shows the equivalent S_{Hmax} orientations calculated from the DIF's only; a total of 71 DIF's were identified on borehole image logs from 11 wells.

5.4. Presentation of statistical data

The authors prefer to use a number weighted method to calculate circular standard deviations from the breakout data.

Table 6
Distribution of breakout observations with depth per category.

Depth (m)	Number of breakouts				Total
	Category				
	1	2	3	4	
0–500	13	1	45	11	70
500–1000	13	38	58	2	111
1000–1500	13	45	3	0	61
1500–2000	6	0	4	0	10

When analysing data from dual-caliper tools it is easy to interpret non stress-related features as breakouts (Heidbach et al., 2010). Due to these problems the use of length weighted circular statistics is vital to avoid misinterpreting the stress field orientation (Sperner et al., 2003). However the greater vertical resolution of borehole image logging means that the number of discrete breakouts identified increases while simultaneously decreasing the overall recorded breakout length over a given interval. Fig. 13 shows two breakouts between 702.4 m and 705.5 m with lengths of 1.4 m and 0.9 m respectively. A different unit can clearly be seen between these two breakouts, most likely a different facies with a higher clay content. A similar effect can also be seen with tensile fractures (Fig. 3) which appear to terminate at a unit with a higher resistivity, which itself has a clear breakout. This is suggestive of a high degree of lithological control on breakout formation within the UK PCM. If there is a process controlling the length of an individual breakout then a length weighted approach may not be the most appropriate method to calculate circular standard deviations within such strata.

This study carefully assessed borehole deformation from both breakouts and DIF's to correctly determine the in-situ stress orientation. However no single borehole available on the UK landmass has all of the information necessary to calculate a stress magnitude. Whilst breakout widths can be calculated for any well with high resolution boreholes images (our Categories 1 and 2), no well interpreted for this study also has the Unconfined Compressive Strength and pore pressure data necessary to accurately calculate stress magnitudes.

5.5. Other stress orientation identifiers

Fig. 8 shows a summary rose diagram showing all observed breakout orientations from this study plotted as S_{Hmax} orientations. These data collectively produce a mean S_{Hmax} orientation of NW–SE. This is consistent with that identified by Evans and Brereton (1990) but with significantly reduced deviation. The results show clearly that while the use of borehole image logs have not significantly altered the current state of understanding regarding the in-situ stress orientations in the region, the associated uncertainties inherent in the other datasets have been significantly reduced. Use of borehole imaging logs to identify stress orientations from sedimentary strata at depths more relevant to UK unconventional reservoir development are perhaps more appropriate to use than deeper earthquake focal mechanism data or near-surface over-coring techniques. The reduced circular standard deviation and unambiguity of imaged and observed features is also significantly improved relative to previous dual-caliper logs studies (Evans and Brereton, 1990). However the results presented in this paper represent a significant reduction in uncertainty greatly reducing the range of possible S_{HMax} orientations.

6. Conclusions

Renewed interest in the in-situ stress field within the

sedimentary successions of the UK is motivated by recent exploration activities seeking to exploit onshore unconventional hydrocarbon resources. It is envisaged that potential shale-gas resources will be exploited through a combination of deviated drilling and hydraulic fracture operations.

While previous studies have stated a regional S_{Hmax} orientation of approximately NW–SE using borehole breakout analysis from dual-caliper logs (Evans and Brereton, 1990), earthquake focal mechanisms (Baptie, 2010) and near-surface overcoring techniques (Bigby et al., 1992; Cartwright, 1997), this study has sought to utilise high quality borehole image logs to elucidate the orientation of S_{Hmax} with a greater degree of confidence and at depths relevant to the exploitation of unconventional hydrocarbons in the UK. In consequence, this study concentrates on identifying and quantifying those intervals which have specifically shown evidence of breakout formation. Only those sections where the explicit presence of breakouts can be demonstrated against a set of clearly defined analysis criteria were then included. The presence of these breakouts and the orientation of S_{Hmax} calculated from them are therefore both repeatable and defensible.

Where geological understanding of the in-situ stress field using downhole measurement tools is required, it is clear that only imaging logs with high borehole wall coverage provide an adequate understanding of well bore failure processes. Although the mean orientations of S_{Hmax} presented are comparable to the earlier study of borehole breakouts (Evans and Brereton, 1990), the results presented here offer a significant reduction in uncertainty. This reduction is a consequence of several factors:

- Greater availability and accessibility of relevant data.
- Availability of borehole imaging data.
- Better quality assurance of data and associated metadata.
- Systematic exclusion of data from boreholes that are significantly deviated from vertical.
- Improved interpretation techniques, focussed on the identification and analysis of specific observed features rather than aggregated borehole measurements.

The combined results for all breakouts interpreted for this study provide a mean S_{Hmax} orientation of 150.91° with a circular standard deviation of 13.07°. The statistics for categories of imaging tools are shown in Table 4, the mean S_{Hmax} orientation for each category falls within ±10° of this with circular standard deviations ranging from 5 to 16°. Fig. 14 shows that the orientations of S_{Hmax} are also consistent with depth. The general agreement with the observed orientations from published earthquake focal measurements suggests that the crustal stresses at deeper seismogenic depths are being transmitted effectively into the shallower sedimentary succession.

The data sufficient to calculate stress magnitudes is not available for any of the wells with borehole imaging. Across the UK there are only a limited number of leak off tests, hydraulic fracturing and overcoring measurements available that can be used to calculate magnitudes. This paper confirms that the stress orientation is essentially uniform through the Triassic and Carboniferous strata of northern and central England. Additional data can subsequently be acquired, through rock test data from not yet released wells.

6.1. Policy implications and recommendations

The needs for hydraulic fracturing operations to allow the development of unconventional hydrocarbon reservoirs has proven controversial, especially given the potential for facilitating leakage of natural gas into drinking water aquifer discussed in Davies et al. (2014). This controversy has been further exacerbated in the UK following induced seismicity at Preese Hall, Lancashire, in 2010.

Existing studies of in-situ stress orientation in the UK have proven wholly inadequate for planning for hydraulic fracturing operations. Regulation of the use of this technique in the UK will require clear planning prior to regulatory approval of any such activities, including consideration of the in-situ stress field around the borehole. This study highlights that dual-caliper logging data are of insufficient resolution to correctly identify the necessary stress indicators. Only well developed borehole breakout, visible over many metres, can be identified from dual-caliper logs whilst DIFs are not visible at all.

Therefore it is the recommendation of the authors that regulators in the United Kingdom, and other similar geological settings, make acquisition of high-resolution borehole imaging mandatory for assessment of unconventional reservoirs. This is due the increased resolution in identifying stress field indicators which will reduce the uncertainty in the orientation of the in-situ stress field. This data must be interpreted prior to the commencement of any hydraulic fracturing operation. This recommendation can only be discounted where other tests of equal or greater accuracy can be shown to have been undertaken. Under UK conditions assessment of in-situ stress through dual-caliper data should not be deemed a sufficient alternative.

It is a further recommendation that the results from any operator are made public so that a database of in-situ stress orientations, and if available magnitudes, can be collated to the benefit of operators and regulators alike. In other parts of the world where boreholes are drilled much deeper or in more active tectonic settings (eg Alpine Forelands) dual-caliper logs may prove sufficient.

Acknowledgements

This paper is published with the permission of the Executive Director of the British Geological Survey. It was funded by BGS National Capability funding from NERC.

Contains Ordnance Survey data © Crown copyright and database rights. All rights reserved [2015] Ordnance Survey [100021290 EUL], Use of this data is subject to terms and conditions. Borehole Imaging displayed using Landmark RECALL software.

The authors wish to thank Oliver Heidbach and an anonymous reviewer for constructive comments to improve this manuscript plus the following colleagues for their advice: Rob Cuss, Helen Reeves, Jim Riding and Fiona McEvoy.

Appendix A. Supplementary data

Supplementary data related to this article can be found at http://dx.doi.org/10.1016/j.marpetgeo.2016.02.012.

References

Andrews, I.J., 2013. The Carboniferous Bowland Shale Gas Study: Geology and Resource Estimation. British Geological Survey for Department of Energy and Climate Change, London, UK.

Baptie, B., 2010. Seismogenesis and state of stress in the UK. Tectonophysics 482 (1–4), 150–159. http://dx.doi.org/10.1016/j.tecto.2009.10.006.

Becker, A., Davenport, C.A., 2001. Contemporary in situ stress determination at three sites in Scotland and northern England. J. Struct. Geol. 23, 407–419.

Bell, J.S., Gough, D.I., 1979. Northeast-Southwest compressive stress in Alberta: evidence from oil wells. Earth Planet. Sci. Lett. 45, 475–482.

Bickle, M., Goodman, D., Mair, R., Roberts, R., Selley, R.C., Shipton, Z., Thomas, H., Younger, P., 2012. Shale Gas Extraction in the UK: a Review of Hydraulic Fracturing. Royal Society & Royal Academy of Engineering, p. 105. royalsociety.org/uploadedFiles/Royal_Society_Content/policy/projects/shale-gas/2012-06-28-Shale-gas.pdf.

Bigby, D.N., Cassie, J.W., Ledger, A.R., 1992. Absolute stress and stress change measurements in British Coal Measures. In: Hudson, J.A. (Ed.), Rock Characterisation: Proceedings of the International Symposium on Rock Stress. United Kingdom, Chester, pp. 390–395.

British Geological Survey, 2015. Rock Stress. http://mapapps.bgs.ac.uk/rockstress/home.html.
Brereton, N.R., 1991. NIREX - Dounreay Structural Geology JIT. Rock stress analysis from borehole breakouts - Dounreay 1 : British Geological Survey report WK/91/013, p. 9.
Brudy, M., Zoback, M.D., 1999. Drilling-induced tensile wall-fractures: Implications for determination of in-situ stress orientation and magnitude. Int. J. Rock Mech. 36, 191–215.
Cartwright, P.B., 1997. A review of recent in-situ stress measurements in the United Kingdom. In: Sugawara, K., Obara, Y. (Eds.), 1997, Rock Stress: Proceedings of the International Symposium on Rock Stress, Kumamoto, Japan, pp. 469–474.
Cartwright, C.E., 2015. Manipulation of UK 2011 National Census Data (Personal Communication).
Davies, R.J., Almond, S., Ward, R.S., Jackson, R.B., Adams, C., Worrall, F., Herringshaw, L.G., Gluyas, J.G., Whitehead, M.A., 2014. Oil and gas wells and their integrity: Implications for shale and unconventional resource exploitation. September 2014 Mar. Petrol. Geol. 56, 239–254. http://dx.doi.org/10.1016/j.marpetgeo.2014.03.001.
Ekstrom, M.P., Dahan, C., Chen, M.-Y., Lloyd, P., Rossi, D.J., 1987. Formation imaging with microelectrical scanning arrays. Log. Anal. 28, 294–306.
Emmermann, R., Lauterjung, J., 1997. The German Continental deep drilling program KTB: overview and major results. J. Geophys. Res. 102 (B8), 18179–18201. http://dx.doi.org/10.1029/96JB03945.
Evans, C.J., 1987. Crustal Stress in the United Kingdom: Investigation of the Geothermal Potential of the U.K. British Geological Survey Report. WJ/GE/87/008.
Evans, C.J., Brereton, N.R., 1990. In situ crustal stress in the United Kingdom from borehole breakouts. In: Hurst, A., Lovell, M.A., Morton, A.C. (Eds.), Geological Applications of Wireline Logs: Geological Society of London Special Publication No. 48, pp. 327–338. http://dx.doi.org/10.1144/GSL.SP.1990.048.01.27.
Evans, D.J., Kingdon, A., Hough, E., Reynolds, W., Heitman, N., 2012. First account of resistivity borehole micro-imaging (FMI) to assess the sedimentology and structure of the Preesall Halite, NW England : implications for gas storage and wider applications in CCS caprock assessment. J. Geol. Soc. 169 (5), 587–592. http://dx.doi.org/10.1144/0016-76492011-143.
Farmer, I.W., Kemeny, J.M., 1992. Deficiencies in rock test data. In: Hudson, J.A. (Ed.), Rock Characterisation: Proceedings of the International Symposium on Rock Stress, Chester, United Kingdom, pp. 298–303.
Fuchs, K., Müller, B., 2001. World Stress Map of the Earth: a ket to tectonic processes and technological applications. Naturwissenschaften 88, 357–371.
Gaillot, P., Brewer, T., Pezard, P., Yeh, E.-C., 2007. Contribution of borehole digital imagery in core-log-seismic integration, 2007. Sci. Drill. 5, 50–53. http://dx.doi.org/10.2204/iodp.sd.5.07.2007.
Garcia-Carballido, Carmen, Boon, Jeannette, Tso, Nancy, 2010. Data management and quality control of dipmeter and borehole image log data. In: Poppelreiter, M., Garcia-Carballido, C., Kraaijveld, M.A. (Eds.), 2010. Dipmeter and Borehole Image Log Technology. American Association of Petroleum Geologists, Memoir 92, pp. 39–49. ISBN 10: 089181373X ISBN 13: 9780891813736.
Green, C.A., Styles, P., Baptie, B.J., 2012. Preese Hall Shale Gas Fracturing: Review & Recommendations for Induced Seismic Mitigation. Induced Seismicity Mitigation Report. Department of Energy & Climate Change. https://www.gov.uk/government/uploads/system/uploads/attachment_data/file/15745/5075-preese-hall-shale-gas-fracturing-review.pdf.
Gölke, M., Coblentz, D., 1996. Origins of the European regional stress field. Tectonophysics 266, 11–24.
Heidbach, O., Barth, A., Connolly, P., Fuchs, K., Müller, B., Reinecker, J., Sperner, B., Tingay, M., Wenzel, F., 2004. Stress maps in a minute: the 2004 world stress map release. Eos Trans. 85 (49), 521–529.
Heidbach, O., Tingay, M., Barth, A., Reinecker, J., Kurfeß, D., Müller, B., 2008. The World Stress Map Database Release 2008. http://dx.doi.org/10.1594/GFZ.WSM.Rel2008.
Heidbach, O., Tingay, M., Barth, A., Reinecker, J., Kurfeß, D., Müller, B., 2010. Global crustal stress pattern based on the World Stress Map database release 2008. Tectonophysics 482 (1–4), 3–15.
Hillis, R.R., Nelson, E.J., 2005. In situ stresses in the North Sea and their applications: petroleum geomechanics from exploration to development. In: Better Recovery through Better Reservoir Characterization: Petroleum Geology Conference Series, 6, pp. 551–564. http://dx.doi.org/10.1144/0060551.
Klein, R.J., Barr, M.V., 1986. Regional state of stress in Western Europe. In: Stephansson, O. (Ed.), Proceedings of the International Symposium on Rock Stress and Rock Stress Measurements, Stockholm, 1–3 September 1986. Centek, Lulea, pp. 33–44.
Leeman, E.R., Hayes, D.J., 1966. A technique for determining the complete state of stress in rock using a single borehole. In: Proceedings of the 1st Congress of the International Society of Rock Mechanics, Lisbon, Part 2, pp. 17–23.
Mastin, L., 1988. Effect of Borehole Deviation on Breakout Orientations. J. Geophys. Res. Solid Earth (1978–2012) 90 (B8), 9187–9195.
Mardia, K.V., 1972. Statistics of Directional Data: Probability and Mathematical Statistics. Academic Press, London, p. 357.
Moos, D., Zoback, M.D., 1990. Utilization of observations of well bore failure to constrain the orientation and magnitude of crustal stresses: application to continental, deep sea drilling project, and ocean drilling program boreholes. J. Geophys. Res. 95 (B6), 9305–9325. http://dx.doi.org/10.1029/JB095iB06p09305.
Nirex, 1997. Sellafield Geological and Hydrogeological Investigations: Assessment of In-situ Stress Field at Sellafield. Nirex Report S/97/003.
Office for National Statistics, 2011. Census: Aggregate Data (England and Wales). UK Data Service Census Support. http://infuse.mimas.ac.uk.
Paillet, F.L., Barton, C., Luthi, S., Rambow, F., Zemanek, J., 1990. Borehole Imaging. SPWLA Reprint Series. Society of Professional Well Log Analysts, Houston, Tex.
Plumb, R.A., Hickman, S.H., 1985. Stress-induced borehole elongation: a comparison between the four-arm dipmeter and the borehole televiewer in the Auburn geothermal well. J. Geophys. Res. 90 (B7), 5513–5521.
Prensky, S.E., 1999. Advances in borehole imaging technology and applications. In: Lovell, M.A., Williamson, G., Harvey, P.K. (Eds.), 1999. Borehole Imaging: Applications and Case Histories. Geological Society, London, pp. 1–43. http://dx.doi.org/10.1144/GSL.SP.1999.159.01.01. Special Publications, 159.
Reeves, Helen J., 2002. The Effect of Stress & Fractures on Fluid Flow in Crystalline Rocks. Durham University, Cumbria, UK. Doctoral thesis. http://etheses.dur.ac.uk/1076/.
Reinecker, J., Tingay, M., Müller, B., 2003. Borehole Breakout Analysis from Four-arm Caliper Logs, World Stress Map Project. WSM. http://dc-app3-14.gfz-potsdam.de/pub/guidelines/WSM_analysis_guideline_breakout_caliper.pdf.
Reinecker, J., Tingay, M., Müller, B., Heidbach, O., 2010. Present-day stress orientation in the Molasse Basin. Tectonophys 462 (1–4). http://dx.doi.org/10.1016/j.tecto.2009.1007.1021.
Reiter, K., Heidbach, O., Moeck, I., Schmitt, D., Hauck, C., 2014. Crustal stress field pattern of Canada. Tectonophys. 636, 1111–1124. http://dx.doi.org/10.1016/j.tecto.2014.1008.1006.
Sathar, S., Reeves, H.J., Cuss, R.J., Harrington, J.F., 2012. The role of stress history on the flow of fluids through fractures. Mineral. Mag. Dec. 2012 76 (8), 3165–3177.
Smith, N., Turner, P., Williams, G., 2010. UK data and analysis for shale gas prospectivity. In: Vining, B.A., Pickering, S.C. (Eds.), Petroleum Geology: from Mature Basins to New Frontiers: Proceedings of the 7th Petroleum Geology Conference. Geological Society, London, pp. 1087–1098.
Sperner, B., Müller, B., Heidbach, O., Delvaux, D., Reinecker, J., Fuchs, K., 2003. Tectonic stress in the Earth's crust: Advances in the World Stress Map Project. In: Nieuwland, D. (Ed.), New Insights into Structural Interpretation and Modeling, pp. 101–116. Geol. Soc. Spec. Publ., 212.
Tingay, M., Reinecker, J., Müller, B., 2008. Borehole breakout and drilling-induced fracture analysis from image logs [online]. In: World Stress Map Project—guidelines: Image Logs, Helmholtz Cent. Potsdam. GFZ German Research Centre for Geosciences, Potsdam, Germany. http://dc-app3-14.gfz-potsdam.de/pub/guidelines/WSM_analysis_guideline_breakout_image.pdf.
Tingay, M., Morley, C., King, R., Hillis, R., Coblentz, D., Hall, R., 2010. Present-day stress field of Southeast Asia. Tectonophysics 482, 92–104. http://dx.doi.org/10.1016/j.tecto.2009.06.019.
U.S. Census Bureau, 2014. Table 1. Annual Estimates of the Resident Population for the United States, Regions, States, and Puerto Rico: April 1, 2010 to July 1, 2014 (CSV).
Williams, J.D.O., Holloway, S., Williams, G.A., 2014. Pressure constraints on the CO2 storage capacity of the saline water-bearing parts of the Bunter Sandstone Formation in the UK Southern North Sea. Pet. Geosci. 20, 155–167.
Williams, J.D.O., Fellgett, M.W., Kingdon, A., Williams, P.J., 2015. In-situ stress orientations in the UK Southern North Sea: Regional trends, deviations and detachment of the post- Zechstein stress field. Mar. Petrol. Geol. 67, 769–784. http://dx.doi.org/10.1016/j.marpetgeo.2015.06.008.
Zoback, M.D., Moos, D., Mastin, L., Anderson, R.N., 1985. Well bore breakouts and in situ stress. J. Geophys. Res. Solid Earth (1978–2012) 90 (B7), 5523–5530.
Zoback, M.L., Zoback, M.D., Adams, J., Assumpcao, M., Bell, S., Bergman, E.A., Blumling, P., Brereton, N.R., Denham, D., Ding, J., Fuchs, K., Gay, N., Gregersen, S., Gupta, H.K., Gvishiani, A., Jacob, K., Klein, R., Knoll, P., Magee, M., Mercier, J.L., Müller, B.C., Paquin, k., Rajendran, K., Stephansson, O., Suarez, M., Suter, M., Udias, A., XU, Z.H., Zhizhin, M., 1989. Global patterns of tectonic stress. Nature 341, 291–298.